

# Multidimensional infrared spectroscopy for molecular vibrational modes with dipolar interactions, anharmonicity, and nonlinearity of dipole moments and polarizability

Kim Hyeon-Deuk<sup>a)</sup> and Yoshitaka Tanimura

*Department of Chemistry, Kyoto University, Kyoto 606-8502, Japan*

(Received 31 August 2005; accepted 12 October 2005; published online 14 December 2005; publisher error corrected 20 January 2006)

We present an analytical expression for the linear and nonlinear infrared spectra of interacting molecular vibrational motions. Each of the molecular modes is explicitly represented by a classical damped oscillator on an anharmonic multidimensional potential-energy surface. The two essential interactions, the dipole-dipole (DD) and the dipole-induced-dipole (DID) interactions, are taken into account, and each dipole moment and polarizability are expanded to nonlinear order with respect to the nuclear vibrational coordinate. Our analytical treatment leads to expressions for the contributions of anharmonicity, DD and DID interactions, and the nonlinearity of dipole moments and polarizability elements to the one-, two-, and three-dimensional spectra as separated terms, which allows us to discuss the relative importance of these respective contributions. We can calculate multidimensional signals for various configurations of molecules interacting through DD and DID interactions for different material parameters over the whole range of frequencies. We demonstrate that contributions from the DD and DID interactions and anharmonicity are separately detectable through the third-order three-dimensional IR spectroscopy, whereas they cannot be distinguished from each other in either the linear or the second-order IR spectroscopies. The possibility of obtaining the intra- or intermolecular structural information from multidimensional spectra is also discussed. © 2005 American Institute of Physics. [DOI: [10.1063/1.2134702](https://doi.org/10.1063/1.2134702)]

## I. INTRODUCTION

Multidimensional vibrational spectroscopies such as the fifth-order Raman<sup>1-4</sup> and the third-order infrared (IR) spectroscopies<sup>5-7</sup> are powerful methods to explore the dynamics and structures of molecules in complex systems. The main advantage of these spectroscopies is due to the sensitivity of multitime correlation functions to anharmonic vibrational motions. Such motions are hard to detect in conventional spectroscopies, but contribute in the leading order to the signals detected by fifth-order Raman and third-order IR spectroscopies.<sup>8,9</sup> In third-order IR experiments, femtosecond phase-controlled IR pulses are available to obtain heterodyne-detected signal fields from samples.<sup>5</sup> The two-dimensional (2D) Fourier plots obtained from the three-pulse vibrational-echo technique have been applied to peptide molecules, e.g., *N*-methylacetamide, for detecting conformational information.<sup>10-13</sup> Some investigations were also conducted on a part of larger molecules, an  $\alpha$  helix and a  $\beta$  sheet.<sup>14,15</sup> Several third-order IR experiments were also performed to evaluate lifetimes of H bonds<sup>16-19</sup> or relaxation times of molecular vibrations in solvents.<sup>7</sup>

In contrast to common practice in the third-order electronically resonant spectroscopies such as pump-probe or photon-echo measurements, the rotating wave approximation (RWA) and the phase-matching condition cannot be adequately applied to vibrational spectroscopies where resonat-

ing frequencies are much smaller than electronically resonant ones.<sup>20</sup> Interactions between vibrational modes, which should be defined by molecular coordinates, exhibit complicated forms. Therefore, descriptions of a Hamiltonian system by means of vibrational energy levels do not seem beneficial and are sometimes inaccurate for the case of vibrational spectroscopy. However, theoretical studies of 2D IR spectroscopy based on a coordinate representation which does not need the RWA were carried out only for single mode cases<sup>1,8,21-23</sup> or multimode cases, but with the limited forms of interactions.<sup>24-26</sup> The aim of this paper is to present explicit analytical expressions with the consideration of such important effects as the anharmonicity of vibrational potentials, the damping constant, the nonlinearity of molecular dipole moments and polarizability elements, and the interactions between dipoles, specifically dipole-dipole (DD) and dipole-induced-dipole (DID) interactions. Their dipole interactions play major roles to determine a signal profile in the third-order IR vibrational spectroscopy.

It has been recognized that interactions between dipoles are a key for the determination of molecular structures. As was suggested by Okumura *et al.*, the DID interaction can be used to determine molecular structures in the 2D Raman spectroscopy.<sup>27</sup> However, such experiments have been carried out by means of the third-order IR spectroscopy, since 2D Raman signals are difficult to obtain owing to cascading effects<sup>28</sup> and vibrational modes in biomolecules of interest usually possess IR-active dipoles such as C=O or N-H bond.<sup>13-15</sup> Actually, there have been several studies on the

<sup>a)</sup>Electronic mail: kim@kuchem.kyoto-u.ac.jp

third-order IR spectroscopy of peptides by *ab initio* calculations and molecular-dynamics (MD) simulations with the help of response function theory.<sup>29–33</sup> Hahn *et al.* demonstrated by an *ab initio* calculation that the intensity of the DID interaction is almost proportional to the third inverse power of distance between dipoles.<sup>34</sup>

Although measuring the third-order IR signal is experimentally easier than measuring the fifth-order Raman one, the reverse is true theoretically. The reason is that the third-order IR signal is defined by a higher-order four-body correlation function which includes more complex interactions between dipoles.<sup>35,36</sup> Nevertheless, theoretical attempts to interpret nonlinear IR spectroscopy through the interactions between dipoles have been performed in several ways. A vibrational-energy-level model based on a quantum picture was often employed to reduce structural information of a macromolecule such as a biomolecule.<sup>37–39</sup> There have been attempts to detect an angular structure between dipoles inside a molecule.<sup>40,41</sup> However, the energy-level model is rather phenomenological, especially when one introduces relaxation or dephasing processes or employs unverified approximations such as the RWA. Thus, such modeling does not usually give any clear molecular interpretation. Alternatively, models in the molecular coordinate representation have been investigated to describe the third-order IR spectroscopy. Cho formulated an IR-IR-visible spectroscopy, including anharmonicity and a part of the DID and DD interactions.<sup>24</sup> Park and Cho obtained expressions for the third-order IR signal from a diagrammatic expansion approach.<sup>25</sup> They suggested a way to determine structures of molecules through the third-order coefficient which came from a DIDID interaction, but their results were limited in the particular case when the second-order coefficient of expanded dipoles which corresponds to the DID interaction becomes zero. This means that they cannot extract the effects of the DID interaction explicitly, which is one of the differences of their results from the results reported in this paper. In addition, our explicit expression allows us to identify the effects of the DID interaction, and the expanded dipole coefficients separately. Our model also takes into account the DD interaction and the angular configurations which play an important role in the third-order IR spectroscopy.

In this paper, we derive analytical expressions for the third-order IR response functions based on the molecular coordinate model. We take into account all explicit contributions from the nonlinear coefficients, the DID interaction, the DD interaction, and the anharmonicity for any three-dimensional configurations of a molecular pair (see Fig. 1), and derive each explicit contribution as separated terms in the third-order IR signal. We demonstrate that, even in complex systems where the above effects are not all negligible, the third-order IR spectroscopy has an ability to separately detect contributions from DID interactions, DD interactions, or the anharmonicity. This finding has never been reported in previous studies. We also consider how structural information can be derived from the DID and DD interactions. Additionally, we have developed a computer program based on the analytical expressions derived in this paper.<sup>42</sup> This program can be used as a handy tool to analyze the third-order

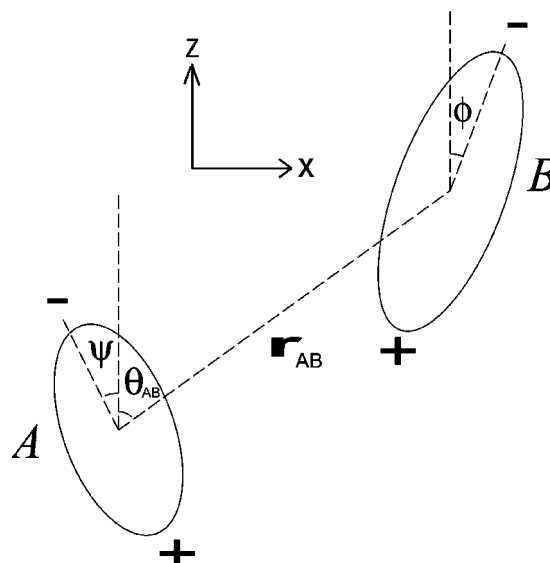


FIG. 1. A pair of dipoles *A* and *B* which interact with each other under an external electric field along the *z* axis.

multidimensional signal as a function of molecular parameters such as the dipole moments and polarizability elements, the damping constants of molecular vibration, and the potential surfaces expressed by molecular coordinates. Furthermore, the DD and DID interactions are included as functions of the configurational parameters depicted in Fig. 1. This program will be helpful for interpreting the third-order IR signals obtained from experiments or simulations and for understanding the physical origins of each peak appearing in the spectrum.

The paper is organized as follows. In Sec. II, we introduce equations of motion based on a model for interacting IR-active vibrational modes. The corresponding solutions are shown in Sec. III. In Secs. IV and V, we briefly summarize the formulation and derive the first-, second-, and third-order response functions. Representative results of the first-, second-, and 2D third-order IR spectroscopy are presented in Sec. VI. Section VII is devoted to the discussion and summary.

## II. EQUATIONS OF MOTION FOR INTERACTING MOLECULAR VIBRATION MODES: A FORCED OSCILLATOR PICTURE

We consider the two vibrational modes *A* and *B* interacting with each other in the presence of an electric field. We denote the nuclear vibrational coordinate of each mode by  $q_A = q_A(t)$  and  $q_B = q_B(t)$ , and their effective masses by  $m_A$  and  $m_B$ . We describe the motion of each vibrational mode by a damped oscillator under external forces. The equations of motion are given as

$$\frac{d^2 q_A}{dt^2} + \gamma_A \frac{dq_A}{dt} + \Omega_A^2 q_A = \frac{f_A(q_A, q_B) + f'_A(q_A, q_B)}{m_A} \quad (1)$$

and

$$\frac{d^2 q_B}{dt^2} + \gamma_B \frac{dq_B}{dt} + \Omega_B^2 q_B = \frac{f_B(q_A, q_B) + f'_B(q_A, q_B)}{m_B}, \quad (2)$$

where  $\Omega_S$  and  $\gamma_S$  denote the frequency and dissipation coefficient of the vibrational mode  $S=A$  or  $B$ , respectively.<sup>7</sup>

The forces on the right-hand side of the above equations correspond to the force from the dipolar interactions

$$f_S(q_A, q_B) = - \frac{\partial V(q_A, q_B)}{\partial q_S} \quad (3)$$

and the force from the anharmonicity

$$f'_S(q_A, q_B) = - \frac{\partial U'_S(q_S)}{\partial q_S} - \frac{\partial U_{AN}(q_A, q_B)}{\partial q_S}, \quad (4)$$

respectively. Here, the anharmonic potential function is defined as

$$U'_S(q_S) = - \frac{V_S^{(3)}}{6} q_S^3 - \frac{V_S^{(4)}}{24} q_S^4 \quad (5)$$

for  $S=A$  or  $B$ .  $V_S^{(3)}$  and  $V_S^{(4)}$  are the cubic and quadratic anharmonicities of the vibrational potential for the mode  $S$ , respectively. The last term on the right-hand side of Eq. (4) corresponds to the anharmonic mode-mode coupling potential function

$$U_{AN}(q_A, q_B) = - \frac{V_{AB}^{(3)}}{2} q_A q_B^2 - \frac{V_{BA}^{(3)}}{2} q_A^2 q_B - \frac{V_{AB}^{(4)}}{4} q_A^2 q_B^2 - \frac{V_{AB}^{(4)}}{6} q_A q_B^3 - \frac{V_{BA}^{(4)}}{6} q_A^3 q_B, \quad (6)$$

where  $V_{AB}^{(n)}$  and  $V_{BA}^{(n)}$  represent the  $n$ th-order anharmonic coupling strength and  $V_{AB}^{(4)}$  is the fourth-order anharmonic coupling coefficient.

Suppose that modes  $A$  and  $B$  have associated dipole moments. If a dipole pair  $A$ - $B$  is isolated from other dipole pairs or if their vibrational frequencies are quite different from the other surrounding modes, such as solvent modes, the dipolar interactions between dipoles  $A$  and  $B$  play essential roles in their intra- or intermolecular interactions. The explicit potential function from dipole interactions in Eq. (3) is written as

$$V(q_A, q_B) = I_{\text{ex}} + I_{\text{DID}} + I_{\text{DD}}, \quad (7)$$

where

$$I_{\text{ex}} = I_{\text{ex}}(q_A, q_B) \equiv - \{ \boldsymbol{\mu}_A^p + \boldsymbol{\mu}_A \} \cdot \mathbf{E}_{\text{ex}}(t, \mathbf{r}_A) - \{ \boldsymbol{\mu}_B^p + \boldsymbol{\mu}_B \} \cdot \mathbf{E}_{\text{ex}}(t, \mathbf{r}_B), \quad (8)$$

$$I_{\text{DID}} = I_{\text{DID}}(q_A, q_B) \equiv - \frac{1}{2} \mathbf{E}_{\text{ex}}(t, \mathbf{r}_A) \cdot \boldsymbol{\alpha}_A \mathbf{T}_{AB} \cdot \boldsymbol{\mu}_B^{\text{tot}} - \frac{1}{2} \mathbf{E}_{\text{ex}}(t, \mathbf{r}_B) \cdot \boldsymbol{\alpha}_B \mathbf{T}_{AB} \cdot \boldsymbol{\mu}_A^{\text{tot}}, \quad (9)$$

and

$$I_{\text{DD}} = I_{\text{DD}}(q_A, q_B) \equiv - \boldsymbol{\mu}_A^{\text{tot}} \cdot \mathbf{D}_{AB} \cdot \boldsymbol{\mu}_B^{\text{tot}}. \quad (10)$$

Here  $\boldsymbol{\mu}_S^p$  and  $\boldsymbol{\mu}_S = \boldsymbol{\mu}_S(q_S)$  for  $S=A$  or  $B$  are the permanent dipole moment and that caused by the vibration coordinate  $q_S$ , respectively.  $\boldsymbol{\alpha}_S = \boldsymbol{\alpha}_S(q_S)$  denotes the polarizability tensor. The total dipole moment is given by

$$\boldsymbol{\mu}_S^{\text{tot}} = \boldsymbol{\mu}_S^{\text{tot}}(q_S, q_{S'}) = \boldsymbol{\mu}_S^p + \boldsymbol{\mu}_S + \boldsymbol{\alpha}_S \mathbf{T}_{AB} \cdot \boldsymbol{\mu}_{S'}^{\text{tot}} \quad (11)$$

for  $(S, S') = (A, B)$  or  $(B, A)$ . The term of  $\mathbf{T}_{AB}$  in Eq. (9) and that of  $\mathbf{D}_{AB}$  in Eq. (10) represent the DD and DID interactions, respectively.

Since the distance between dipoles  $A$  and  $B$ ,  $r_{AB}$ , is smaller than the optical wavelength, the external field  $\mathbf{E}_{\text{ex}}(t, \mathbf{r}_A)$  or  $\mathbf{E}_{\text{ex}}(t, \mathbf{r}_B)$  in Eqs. (8) and (9) can be replaced by  $\mathbf{E}_{\text{ex}}(t, \mathbf{r}_G)$ , where  $\mathbf{r}_G$  denotes the midpoint between the two dipoles. Furthermore, the forms of  $\mathbf{T}_{AB}$  and  $\mathbf{D}_{AB}$  can be expressed as

$$\mathbf{T}_{AB} = \mathbf{D}_{AB} \equiv \frac{3 \hat{\mathbf{r}}_{AB} \hat{\mathbf{r}}_{AB} - \mathbf{I}}{4 \pi \epsilon_0 r_{AB}^3}, \quad (12)$$

where  $\epsilon_0$  is the vacuum dielectric constant and  $\hat{\mathbf{r}}_{AB}$  is the unit vector from the center of dipole  $A$  to the center of dipole  $B$ .<sup>43</sup> It can be assumed that, if the distance between dipoles  $r_{AB}$  is large enough, the higher-order terms of  $\mathbf{T}_{AB}$  and  $\mathbf{D}_{AB}$  in Eq. (12) are negligible. We note that DD and DID interactions are essential for interactions between dipoles, and that other dipole interactions such as the van der Waals interaction which is of order  $O(1/r_{AB}^6)$  are neglected.

We consider a  $x$ - $z$  plane where dipoles  $A$  and  $B$  exist, as is drawn in Fig. 1. Using Eq. (11), the terms of Eq. (7) leads to

$$I_{\text{ex}} = - (\boldsymbol{\mu}_A^p + \boldsymbol{\mu}_A) \mathbf{E}_{\text{ex}}(t, \mathbf{r}_G) \cos \psi - (\boldsymbol{\mu}_B^p + \boldsymbol{\mu}_B) \mathbf{E}_{\text{ex}}(t, \mathbf{r}_G) \cos \phi, \quad (13)$$

$$I_{\text{DID}} = - \frac{1}{2} \mathbf{E}_{\text{ex}}(t, \mathbf{r}_G) \mathbf{T}_{AB} \boldsymbol{\alpha}_A (\boldsymbol{\mu}_B^p + \boldsymbol{\mu}_B) - \frac{1}{2} \mathbf{E}_{\text{ex}}(t, \mathbf{r}_G) \mathbf{T}_{AB} \boldsymbol{\alpha}_B (\boldsymbol{\mu}_A^p + \boldsymbol{\mu}_A), \quad (14)$$

and

$$I_{\text{DD}} = - \mathbf{D}_{AB} (\boldsymbol{\mu}_A^p + \boldsymbol{\mu}_A) (\boldsymbol{\mu}_B^p + \boldsymbol{\mu}_B), \quad (15)$$

to the first order of  $\mathbf{T}_{AB}$  and  $\mathbf{D}_{AB}$ . Here,  $\mathbf{E}_{\text{ex}}(t, \mathbf{r}_G)$  denotes the intensity of an external electric field  $\mathbf{E}_{\text{ex}}(t, \mathbf{r}_G)$  which is parallel to the  $z$  axis.  $\psi$  and  $\phi$  are angles between an electric field and dipoles  $A$  and  $B$  (Fig. 1).  $\mathbf{T}_{AB}$  and  $\mathbf{D}_{AB}$  are obtained as

$$\mathbf{T}_{AB} = \mathbf{D}_{AB} = \frac{\{3 \sin^2 \theta_{AB} - 1\} \sin \psi \sin \phi + \{3 \cos^2 \theta_{AB} - 1\} \cos \psi \cos \phi + 3 \sin \theta_{AB} \cos \theta_{AB} \sin(\psi + \phi)}{4 \pi \epsilon_0 r_{AB}^3}, \quad (16)$$

with  $\theta_{AB}$  shown in Fig. 1. Note that  $\mu_S$  means the magnitude of a dipole moment vector  $\boldsymbol{\mu}_S$  and we set  $\alpha_A^{zx} = \alpha_A \sin \psi$ ,  $\alpha_A^{zz} = \alpha_A \cos \psi$ ,  $\alpha_B^{zx} = \alpha_B \sin \phi$ , and  $\alpha_B^{zz} = \alpha_B \cos \phi$  with  $\alpha_A = \alpha_A(q_A)$  and  $\alpha_B = \alpha_B(q_B)$ .

The specific solution of Eqs. (1) and (2) can be derived as

$$q_S(t) = \int d\tau [f_S(q_A(t-\tau), q_B(t-\tau)) + f'_S(q_A(t-\tau), q_B(t-\tau))] D_S(\tau), \quad (17)$$

where

$$D_S(\tau) \equiv \Theta(\tau) \frac{\exp[-\gamma_S \tau/2]}{m_S \xi_S} \sin \xi_S \tau, \quad (18)$$

with the Heaviside step function  $\Theta(\tau)$  and the effective frequency

$$\xi_S \equiv \sqrt{\Omega_S^2 - \frac{\gamma_S^2}{4}}. \quad (19)$$

The dipole moment and the polarizability can be expanded in the molecular vibration coordinate as

$$\mu_S(t) = \mu_S^{(1)} q_S(t) + \frac{\mu_S^{(2)}}{2} q_S^2(t) + \frac{\mu_S^{(3)}}{6} q_S^3(t) + \dots \quad (20)$$

and

$$\alpha_S(t) = \alpha_S^{(0)} + \alpha_S^{(1)} q_S(t) + \frac{\alpha_S^{(2)}}{2} q_S^2(t) + \frac{\alpha_S^{(3)}}{6} q_S^3(t) + \dots, \quad (21)$$

respectively. Here, we assume that there are no couplings between molecules  $A$  and  $B$  at the level of the dipole moment and polarizability. This is reasonable since  $r_{AB}$  is large enough to regard dipoles  $A$  and  $B$  as localized.

We regard the terms proportional to the higher-order nonlinear coefficients of the expanded dipole moment  $D_{AB} \mu_S^p \mu_S^{(3)}$ ,  $D_{AB} \mu_S^p \mu_S^{(4)}$ , and  $D_{AB} \mu_S^{(1)} \mu_S^{(3)}$  as part of the anharmonicity in  $U_{AN}(q_A, q_B)$  and  $U'(q_S)$ , and eliminate the former contributions from the expression of  $I_{DD}$ . This practice is justified because the above higher-order nonlinear coefficients are usually small in nonlinear spectroscopy, and, moreover, the anharmonicities  $V_S^{(3)}$ ,  $V_S^{(4)}$ , and  $V_{SS'}^{(4)}$  play more essential roles than those coefficients. However, we have not neglected the third-order nonlinearities  $\mu_S^{(3)}$  and  $\alpha_S^{(3)}$  in the terms which include  $E_{\text{ex}}(t, \mathbf{r}_G)$ , since these terms make different contributions to the nonlinear IR spectroscopy.<sup>25,44</sup> With the above assumptions, we substitute Eqs. (20) and (21) into Eqs. (13)–(15) and obtain the explicit forms of  $V(q_A, q_B)$ . Hereafter, we express  $E_{\text{ex}}(t, \mathbf{r}_G)$  only by  $E_{\text{ex}}(t)$  for simplicity.

The vibrational coordinate  $q_S(t)$  can be expanded in orders of the applied external fields  $E_{\text{ex}}(t)$  as

$$q_S(t) = q_S^{(1)}(t) + q_S^{(2)}(t) + q_S^{(3)}(t) + \dots, \quad (22)$$

which holds only when the external electric field is weak enough. It is natural that  $q_S^{(0)} = 0$  because a molecular vibration coordinate is regarded as a renormalized coordinate with no external electric field. With the above expanded expressions, (20)–(22), Eq. (1) leads to the first-order equation of motion of molecule  $A$ ,

$$m_A \left[ \frac{d^2 q_A^{(1)}}{dt^2} + \gamma_A \frac{dq_A^{(1)}}{dt} + \Omega_A^{*2} q_A^{(1)} \right] = E_{\text{ex}}(t) \mu_A^{(1)} \cos \psi + \frac{1}{2} E_{\text{ex}}(t) T_{AB} \Phi_{AB}^{(1,0)} + D_{AB} \mu_A^{(1)} \mu_B^{(1)} q_B^{(1)}, \quad (23)$$

where

$$\Phi_{SS'}^{(n,m)} \equiv \alpha_S^{(n)} \mu_{S'}^{(m)} + \mu_S^{(n)} \alpha_{S'}^{(m)}, \quad (24)$$

with  $\mu_S^{(0)} \equiv \mu_S^p$ , and

$$\Omega_A^{*2} \equiv \Omega_A^2 - \frac{D_{AB}}{m_A} \mu_A^{(2)} \mu_B^p. \quad (25)$$

This equation shows that a specific frequency is modified by the DD interaction. We also mention that dipole configurations such as  $\psi$ ,  $\phi$ ,  $\theta_{AB}$ , and  $r_{AB}$  can be regarded as constants, compared with the molecular dynamics within an ultrafast time scale. Similarly, Eq. (1) leads to the second-order equation of motion,

$$m_A \left[ \frac{d^2 q_A^{(2)}}{dt^2} + \gamma_A \frac{dq_A^{(2)}}{dt} + \Omega_A^{*2} q_A^{(2)} \right] = E_{\text{ex}}(t) \mu_A^{(2)} q_A^{(1)} \cos \psi + \frac{1}{2} E_{\text{ex}}(t) T_{AB} [\Phi_{AB}^{(1,1)} q_B^{(1)} + \Phi_{AB}^{(2,0)} q_A^{(1)}] + D_{AB} \left[ \mu_A^{(1)} \mu_B^{(1)} q_B^{(2)} + \mu_A^{(1)} \mu_B^{(2)} \frac{q_B^{(1)2}}{2} + \mu_A^{(2)} \mu_B^{(1)} q_A^{(1)} q_B^{(1)} \right] + V_A^{(3)} \frac{q_A^{(1)2}}{2} + V_{AB}^{(3)} \frac{q_B^{(1)2}}{2} + V_{BA}^{(3)} q_A^{(1)} q_B^{(1)}. \quad (26)$$

Finally, we can derive the third-order equation of motion from Eq. (1),

$$\begin{aligned}
m_A \left[ \frac{d^2 q_A^{(3)}}{dt^2} + \gamma_A \frac{dq_A^{(3)}}{dt} + \Omega_A^{*2} q_A^{(3)} \right] = E_{\text{ex}}(t) \left[ \mu_A^{(2)} q_A^{(2)} + \frac{\mu_A^{(3)}}{2} q_A^{(1)2} \right] \cos \psi \\
+ \frac{1}{2} E_{\text{ex}}(t) T_{AB} \left[ \Phi_{AB}^{(1,1)} q_B^{(2)} + \Phi_{AB}^{(1,2)} \frac{q_B^{(1)2}}{2} + \Phi_{AB}^{(2,1)} q_A^{(1)} q_B^{(1)} + \Phi_{AB}^{(2,0)} q_A^{(2)} + \Phi_{AB}^{(3,0)} \frac{q_A^{(1)2}}{2} \right] \\
+ D_{AB} \left[ \mu_A^{(1)} \mu_B^{(1)} q_B^{(3)} + \mu_A^{(2)} \mu_B^{(1)} q_A^{(2)} q_B^{(1)} + \mu_A^{(2)} \mu_B^{(1)} q_A^{(1)} q_B^{(2)} + \mu_A^{(2)} \mu_B^{(2)} \frac{q_A^{(1)} q_B^{(1)2}}{2} \right] \\
+ V_{AB}^{(4)} \frac{q_B^{(1)3}}{6} + V_{BA}^{(4)} \frac{q_A^{(1)2} q_B^{(1)}}{2} + V_A^{(4)} \frac{q_A^{(1)3}}{6} + V_{AB}^{(4)} \frac{q_A^{(1)} q_B^{(1)2}}{2} + V_{BA}^{(3)} q_A^{(1)} q_B^{(2)} + V_{BA}^{(3)} q_A^{(2)} q_B^{(1)}. \quad (27)
\end{aligned}$$

Each equation of motion for molecule  $B$  can be obtained by interchanging suffix  $A$  with  $B$  in the above equations.

### III. MOLECULAR VIBRATIONAL COORDINATES

#### A. The first-order solution

With the use of Eq. (17), we have the solution of Eq. (23) as

$$q_S^{(1)}(t) = \int d\tau \left[ E_{\text{ex}}(t-\tau) \mu_S^{(1)} \cos \theta_S + \frac{1}{2} E_{\text{ex}}(t-\tau) T_{AB} \Phi_{SS'}^{(1,0)} + D_{AB} \mu_S^{(1)} \mu_{S'}^{(1)} q_{S'}^{(1)}(t-\tau) \right] D_S(\tau). \quad (28)$$

Note that  $\Omega_S$  of  $\xi_S$ , which appears in  $D_S(\tau)$ , is now replaced by  $\Omega_S^*$  and that  $\theta_S = \psi$  for  $S=A$  and  $\theta_S = \phi$  for  $S=B$ . Substituting the above expression for  $q_{S'}^{(1)}(t)$  into Eq. (28), we obtain the first-order solution

$$\begin{aligned}
q_S^{(1)}(t) = \int d\tau \left[ E_{\text{ex}}(t-\tau) \mu_S^{(1)} \cos \theta_S + \frac{1}{2} E_{\text{ex}}(t-\tau) T_{AB} \Phi_{SS'}^{(1,0)} \right] D_S(\tau) \\
+ \int d\tau \int d\tau' E_{\text{ex}}(t-\tau-\tau') D_{AB} \mu_S^{(1)} \mu_{S'}^{(1)2} \cos \theta_{S'} D_{S'}(\tau') D_S(\tau), \quad (29)
\end{aligned}$$

to linear order in  $T_{AB}$  and  $D_{AB}$ .

#### B. The second-order solution

Similarly, from Eq. (17), the solution of Eq. (26) becomes

$$\begin{aligned}
q_S^{(2)}(t) = \int d\tau \left[ E_{\text{ex}}(t-\tau) \mu_S^{(2)} \cos \theta_S q_S^{(1)}(t-\tau) + \frac{1}{2} E_{\text{ex}}(t-\tau) T_{AB} \{ \Phi_{SS'}^{(1,2)} q_{S'}^{(1)}(t-\tau) + \Phi_{SS'}^{(2,0)} q_S^{(1)}(t-\tau) \} \right. \\
+ D_{AB} \left\{ \mu_S^{(1)} \mu_{S'}^{(1)} q_{S'}^{(2)}(t-\tau) + \mu_S^{(1)} \mu_{S'}^{(2)} \frac{q_{S'}^{(1)2}(t-\tau)}{2} + \mu_S^{(2)} \mu_{S'}^{(1)} q_S^{(1)}(t-\tau) q_{S'}^{(1)}(t-\tau) \right\} \\
+ V_S^{(3)} \frac{q_S^{(1)2}(t-\tau)}{2} V_{SS'}^{(3)} \frac{q_{S'}^{(1)2}(t-\tau)}{2} V_{S'S}^{(3)} q_S^{(1)}(t-\tau) q_{S'}^{(1)}(t-\tau) \left. \right] D_S(\tau). \quad (30)
\end{aligned}$$

Inserting the above form for  $q_{S'}^{(2)}(t)$  and the first-order solutions into Eq. (30), we have the second-order solution as

$$\begin{aligned}
q_S^{(2)}(t) = \mu_S^{(1)} \mu_S^{(2)} \cos^2 \theta_S A_{SS}(t) + \frac{T_{AB}}{2} \{ \Phi_{SS}^{(1,2)} \mu_{S'}^2 + 2\alpha_{S'}^{(0)} \mu_S^{(1)} \mu_S^{(2)} \} \cos \theta_S A_{SS}(t) + \frac{T_{AB}}{2} \Phi_{SS'}^{(1,1)} \mu_{S'}^{(1)} \cos \theta_{S'} A_{S'S}(t) \\
+ D_{AB} \mu_S^{(1)} \mu_S^{(2)} \mu_{S'}^{(1)2} \cos \theta_S \cos \theta_{S'} B_{S'SS}(t) + \frac{D_{AB}}{2} \{ \mu_S^{(1)} \mu_{S'}^{(1)2} \mu_S^{(2)} \cos^2 \theta_{S'} C_{S'S'S}(t) \\
+ 2\mu_S^{(1)} \mu_S^{(2)} \mu_{S'}^{(1)2} \cos \theta_S \cos \theta_{S'} C_{S'SS}(t) \} + D_{AB} \mu_S^{(1)} \mu_{S'}^{(1)2} \mu_S^{(2)} \cos^2 \theta_{S'} F_{S'S'S}(t) + \frac{1}{2} \mu_S^{(1)2} V_S^{(3)} \cos^2 \theta_S C_{SSS}(t) \\
+ \frac{1}{2} \mu_{S'}^{(1)2} V_{S'S}^{(3)} \cos^2 \theta_{S'} C_{S'S'S}(t) + \mu_S^{(1)} \mu_{S'}^{(1)} V_{S'S}^{(3)} \cos \theta_S \cos \theta_{S'} C_{S'SS}(t), \quad (31)
\end{aligned}$$

to linear order in  $T_{AB}$ ,  $D_{AB}$ , and  $V_S^{(3)}$ . Here, we have introduced the following expressions:

$$A_{S'S}(t) \equiv \int d\tau \int d\tau' E_{\text{ex}}(t-\tau) E_{\text{ex}}(t-\tau-\tau') D_{S'}(\tau') D_S(\tau), \quad (32)$$



$$B_{S''S'S}(t) \equiv \int d\tau \int d\tau' \int d\tau'' E_{\text{ex}}(t-\tau) E_{\text{ex}}(t-\tau-\tau'-\tau'') D_{S''}(\tau'') D_{S'}(\tau') D_S(\tau), \quad (33)$$

$$C_{S''S'S}(t) \equiv \int d\tau \int d\tau' \int d\tau'' E_{\text{ex}}(t-\tau-\tau') E_{\text{ex}}(t-\tau-\tau'-\tau'') D_{S''}(\tau'') D_{S'}(\tau') D_S(\tau), \quad (34)$$

and

$$F_{S''S'S}(t) \equiv \int d\tau \int d\tau' \int d\tau'' E_{\text{ex}}(t-\tau-\tau') E_{\text{ex}}(t-\tau-\tau'-\tau'') D_{S''}(\tau'') D_{S'}(\tau') D_S(\tau). \quad (35)$$

### C. The third-order solution

With Eq. (17) being applied, we have the solution of Eq. (27) as

$$\begin{aligned} q_S^{(3)}(t) = & \int d\tau E_{\text{ex}}(t-\tau) \left\{ \mu_S^{(2)} q_S^{(2)}(t-\tau) + \frac{\mu_S^{(3)}}{2} q_S^{(1)2}(t-\tau) \right\} \cos \theta_S D_S(\tau) + \frac{T_{AB}}{2} \int d\tau E_{\text{ex}}(t-\tau) \\ & \times \left[ \Phi_{SS'}^{(1,1)} q_{S'}^{(2)}(t-\tau) + \Phi_{SS'}^{(1,2)} \frac{q_{S'}^{(1)2}(t-\tau)}{2} + \Phi_{SS'}^{(2,1)} q_S^{(1)}(t-\tau) q_{S'}^{(1)}(t-\tau) + \Phi_{SS'}^{(2,0)} q_S^{(2)}(t-\tau) + \Phi_{SS'}^{(3,0)} \frac{q_S^{(1)2}(t-\tau)}{2} \right] D_S(\tau) \\ & + D_{AB} \int d\tau \left\{ \mu_S^{(1)} \mu_{S'}^{(1)} q_{S'}^{(3)}(t-\tau) + \mu_S^{(2)} \mu_{S'}^{(1)} q_S^{(2)}(t-\tau) q_{S'}^{(1)}(t-\tau) + \mu_S^{(2)} \mu_{S'}^{(1)} q_S^{(1)}(t-\tau) q_{S'}^{(2)}(t-\tau) \right. \\ & \left. + \mu_S^{(2)} \mu_{S'}^{(2)} \frac{q_S^{(1)}(t-\tau) q_{S'}^{(1)2}(t-\tau)}{2} \right\} D_S(\tau) + \int d\tau \left\{ V_{SS'}^{(4)} \frac{q_{S'}^{(1)3}(t-\tau)}{6} + V_{S'S}^{(4)} \frac{q_S^{(1)2}(t-\tau) q_{S'}^{(1)}(t-\tau)}{2} + V_S^{(4)} \frac{q_S^{(1)3}(t-\tau)}{6} \right. \\ & \left. + V_{SS'}^{(4)} \frac{q_S^{(1)}(t-\tau) q_{S'}^{(1)2}(t-\tau)}{2} + V_{S'S}^{(3)} q_S^{(1)}(t-\tau) q_{S'}^{(2)}(t-\tau) + V_{S'S}^{(3)} q_S^{(2)}(t-\tau) q_{S'}^{(1)}(t-\tau) \right\} D_S(\tau). \quad (36) \end{aligned}$$

Substituting the above expression for  $q_{S'}^{(3)}(t)$  and the first- and second-order solutions into Eq. (36), we can derive the third-order solution which is written in our Technical Note.<sup>42</sup>

### IV. LINEAR IR SPECTROSCOPY

The dipole moment along the  $z$  axis, which is parallel to the external field and observed in vibrational spectroscopy experiments, can be written as

$$P(t) = \sum_N \frac{\mu_A^{\text{tot}}(t) + \mu_B^{\text{tot}}(t)}{V}, \quad (37)$$

where  $N$  means a number of  $A$  and  $B$  pairs in the sample and  $V$  is the sample volume.  $\mu_S^{\text{tot}}(t)$  denotes a  $z$  component of  $\boldsymbol{\mu}_S^{\text{tot}}$  in Eq. (11). Equation (11) leads to

$$\mu_S^{\text{tot}}(t) = (\mu_S^p + \mu_S(t)) \cos \theta_S + \alpha_S(t) T_{AB} (\mu_{S'}^p + \mu_{S'}(t)), \quad (38)$$

to linear order in  $T_{AB}$ . Substituting Eqs. (20)–(22) for Eq. (38), we obtain the first-order dipole moment of molecule  $S$ ,

$$\mu_S^{\text{tot}(1)}(t) = \mu_S^{(1)} q_S^{(1)}(t) \cos \theta_S + T_{AB} \mu_{S'}^p \alpha_S^{(1)} q_{S'}^{(1)}(t) + T_{AB} \alpha_S^{(0)} \mu_{S'}^{(1)} q_{S'}^{(1)}(t), \quad (39)$$

where the first-order solution  $q_S^{(1)}(t)$  has been already derived in Eq. (29). Therefore, its final form becomes

$$\begin{aligned} \mu_S^{\text{tot}(1)}(t) = & \mu_S^{(1)2} \int d\tau E_{\text{ex}}(t-\tau) D_S(\tau) \cos^2 \theta_S + T_{AB} \left\{ \frac{3}{2} \mu_S^{(1)} \alpha_S^{(1)} \mu_{S'}^p + \frac{\alpha_{S'}^{(0)} \mu_S^{(1)2}}{2} \right\} \int d\tau E_{\text{ex}}(t-\tau) D_S(\tau) \cos \theta_S \\ & + T_{AB} \alpha_S^{(0)} \mu_{S'}^{(1)2} \int d\tau E_{\text{ex}}(t-\tau) D_{S'}(\tau) \cos \theta_{S'} + D_{AB} \mu_S^{(1)2} \mu_{S'}^{(1)2} \int d\tau \int d\tau' E_{\text{ex}}(t-\tau-\tau') D_{S'}(\tau') D_S(\tau) \cos \theta_S \cos \theta_{S'}, \quad (40) \end{aligned}$$

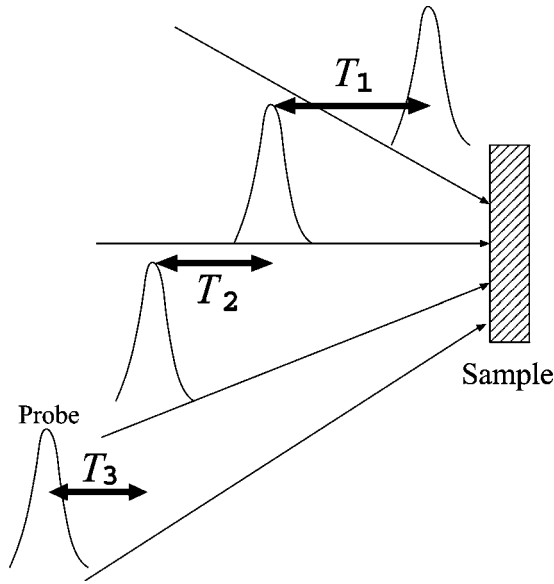


FIG. 2. A schematic description of nonlinear IR spectroscopy. A sample interacts with the first electric field at  $t=0$ , then with the second one at  $t=T_1$ , and finally with the third one at  $t=T_1+T_2$ . The sample radiates an IR field at  $t=T_1+T_2+T_3$ .

to linear order in  $T_{AB}$  and  $D_{AB}$ . For the linear spectroscopy, we define the external electric field  $E_{\text{ex}}(t)$  as

$$E_{\text{ex}}(t) = E_0 \delta(t), \quad (41)$$

where  $E_0$  represents an amplitude of an electric pulse (Fig. 2). We note that the above definition directly generates the first-order response function as follows. Insertion of Eq. (41) into Eq. (40) leads to

$$\begin{aligned} \mu_S^{\text{tot}(1)}(T_1) = E_0 & \left[ \mu_S^{(1)2} D_S(T_1) \cos^2 \theta_S + T_{AB} \right. \\ & \times \left\{ \frac{3}{2} \mu_S^{(1)} \alpha_S^{(1)} \mu_{S'}^p + \frac{\alpha_{S'}^{(0)} \mu_S^{(1)2}}{2} \right\} D_S(T_1) \cos \theta_S \\ & + T_{AB} \alpha_S^{(0)} \mu_{S'}^{(1)2} D_{S'}(T_1) \cos \theta_{S'} \\ & \left. + D_{AB} \mu_S^{(1)2} \mu_{S'}^{(1)2} G_{AB}(T_1) \cos \theta_S \cos \theta_{S'} \right], \quad (42) \end{aligned}$$

where  $G_{AB}(T_1)$  is defined in Appendix A. We can finally derive the first-order response function defined by  $P^{(1)}(T_1) \equiv n_0 E_0 R^{(1)}(T_1)$  as

$$\begin{aligned} R^{(1)}(T_1) = & \mu_A^{(1)2} D_A(T_1) \cos^2 \psi + \mu_B^{(1)2} D_B(T_1) \cos^2 \phi \\ & + \frac{3}{2} \tilde{T}_{AB} D_A(T_1) \cos \psi \mu_A^{(1)} \Phi_{AB}^{(1,0)} \\ & + \frac{3}{2} \tilde{T}_{AB} D_B(T_1) \cos \phi \mu_B^{(1)} \Phi_{AB}^{(0,1)} \\ & + 2 \tilde{D}_{AB} \mu_A^{(1)2} \mu_B^{(1)2} G_{AB}(T_1) \cos \psi \cos \phi \quad (43) \end{aligned}$$

from Eq. (37). Here,  $n_0$  indicates the concentration of A and B pairs.  $\tilde{T}_{AB}$  and  $\tilde{D}_{AB}$  are statistically averaged values of  $T_{AB}$  and  $D_{AB}$ . The first-order spectral density which is observable in the experiments is defined as

$$I^{(1)}(\omega_1) \equiv -i \int_0^\infty e^{i\omega_1 T_1} R^{(1)}(T_1) dT_1, \quad (44)$$

whose explicit expression is given in Appendix B. Results of a representative example will be shown graphically in Sec. VI.

## V. NONLINEAR IR SPECTROSCOPY

### A. The second-order spectroscopy

From Eq. (38) with Eqs. (20)–(22), we obtain the second-order dipole moment of molecule  $S$  as

$$\begin{aligned} \mu_S^{\text{tot}(2)}(t) = & \mu_S^{(1)} q_S^{(2)}(t) \cos \theta_S + \frac{\mu_S^{(2)}}{2} q_S^{(1)2}(t) \cos \theta_S \\ & + T_{AB} \alpha_S^{(1)} \mu_{S'}^p q_S^{(2)}(t) + \frac{T_{AB}}{2} \alpha_S^{(2)} \mu_{S'}^p q_S^{(1)2}(t) \\ & + T_{AB} \alpha_S^{(0)} \mu_{S'}^{(1)} q_S^{(2)}(t) + \frac{T_{AB}}{2} \alpha_S^{(0)} \mu_{S'}^{(2)} q_S^{(1)2}(t) \\ & + T_{AB} \alpha_S^{(1)} \mu_{S'}^{(1)} q_S^{(1)}(t) q_{S'}^{(1)}(t). \quad (45) \end{aligned}$$

Substitution of the expressions in Eqs. (29) and (31) for those in the above equation leads to  $\mu_S^{\text{tot}(2)}(t)$  in Appendix C, whose explicit form has never been obtained in previous studies.<sup>24,25</sup> For the second-order spectroscopy, we define the external electric field  $E_{\text{ex}}(t)$  as

$$E_{\text{ex}}(t) = E_0 \delta(t) + E_0 \delta(t - T_1). \quad (46)$$

(See Fig. 2.) The insertion of Eq. (46) into Eq. (C1) leads to  $\mu_S^{\text{tot}(2)}(T_{12})$ . Note that we denote  $T_{12} \equiv T_1 + T_2$ . Its explicit form is given in Appendix C. From Eq. (37), we can derive the second-order response function defined by  $P^{(2)}(T_{12}) \equiv n_0 E_0^2 R^{(2)}(T_1, T_2)$  as

$$\begin{aligned} R^{(2)}(T_1, T_2) = & N^{(2)}(T_1, T_2) + T^{(2)}(T_1, T_2) + D^{(2)}(T_1, T_2) \\ & + A^{(2)}(T_1, T_2), \quad (47) \end{aligned}$$

where the contributions of the nonlinearity of the dipole moments to  $R^{(2)}(T_1, T_2)$  become

$$\begin{aligned} N^{(2)}(T_1, T_2) \equiv & \mu_A^{(1)2} \mu_A^{(2)} \{ D_A(T_1) D_A(T_2) \\ & + D_A(T_{12}) D_A(T_2) \} \cos^3 \psi + \mu_B^{(1)2} \mu_B^{(2)} \\ & \times \{ D_B(T_1) D_B(T_2) + D_B(T_{12}) D_B(T_2) \} \cos^3 \phi. \quad (48) \end{aligned}$$

The effects of the DID interaction lead to

$$\begin{aligned}
T^{(2)}(T_1, T_2) \equiv & \frac{\tilde{T}_{AB}}{2} \mu_A^{(1)} (2\mu_A^{(2)} \Phi_{AB}^{(1,0)} + \mu_B^p \Phi_{AA}^{(1,2)}) D_A(T_1) D_A(T_2) \cos^2 \psi + \frac{\tilde{T}_{AB}}{2} \mu_B^{(1)} (2\mu_B^{(2)} \Phi_{BA}^{(1,0)} + \mu_A^p \Phi_{BB}^{(1,2)}) D_B(T_1) D_B(T_2) \cos^2 \phi \\
& + \tilde{T}_{AB} \mu_A^{(1)} \{ \Phi_{AA}^{(1,2)} \mu_B^p + \alpha_B^{(0)} \mu_A^{(1)} \mu_A^{(2)} \} D_A(T_1) D_A(T_2) \cos^2 \psi + \tilde{T}_{AB} \mu_B^{(1)} \{ \Phi_{BB}^{(1,2)} \mu_A^p \\
& + \alpha_A^{(0)} \mu_B^{(1)} \mu_B^{(2)} \} D_B(T_1) D_B(T_2) \cos^2 \phi + \tilde{T}_{AB} \alpha_A^{(0)} \mu_B^{(1)2} \mu_B^{(2)} \{ D_A(T_1) D_A(T_2) + D_A(T_1) D_A(T_2) \} \cos^2 \phi \\
& + \tilde{T}_{AB} \alpha_B^{(0)} \mu_A^{(1)2} \mu_A^{(2)} \{ D_B(T_1) D_B(T_2) + D_B(T_1) D_B(T_2) \} \cos^2 \psi + \frac{\tilde{T}_{AB}}{2} \mu_A^{(1)} \mu_B^{(1)} \Phi_{AB}^{(1,1)} \{ D_B(T_1) D_A(T_2) \\
& + D_A(T_1) D_B(T_2) + 2D_A(T_1) D_B(T_2) + 2D_B(T_1) D_A(T_2) \} \cos \psi \cos \phi. \tag{49}
\end{aligned}$$

The contributions of the DD interaction become

$$\begin{aligned}
D^{(2)}(T_1, T_2) \equiv & \frac{\tilde{D}_{AB}}{2} \mu_A^{(1)2} \mu_B^{(1)2} \mu_B^{(2)} \{ 2D_B(T_1) G_{AB}(T_2) + 2G_{AB}(T_1) D_B(T_2) + 2G_{AB}(T_1) D_B(T_2) + 2G_{AB}(T_2) D_B(T_1) \\
& + 2H_{BAB}(T_1, T_2) + H_{BBA}(T_1, T_2) \} \cos \psi \cos^2 \phi + \frac{\tilde{D}_{AB}}{2} \mu_B^{(1)2} \mu_A^{(1)2} \mu_A^{(2)} \{ 2D_A(T_1) G_{AB}(T_2) + 2G_{AB}(T_1) D_A(T_2) \\
& + 2G_{AB}(T_1) D_A(T_2) + 2G_{AB}(T_2) D_A(T_1) + 2H_{ABA}(T_1, T_2) + H_{AAB}(T_1, T_2) \} \cos^2 \psi \cos \phi, \tag{50}
\end{aligned}$$

and the effects of the anharmonicity result in

$$\begin{aligned}
A^{(2)}(T_1, T_2) \equiv & \frac{1}{2} \mu_A^{(1)3} V_A^{(3)} H_{AAA}(T_1, T_2) \cos^3 \psi + \frac{1}{2} \mu_B^{(1)3} V_B^{(3)} H_{BBB}(T_1, T_2) \cos^3 \phi + \frac{1}{2} \mu_A^{(1)} \mu_B^{(1)2} V_{AB}^{(3)} [H_{BBA}(T_1, T_2) \\
& + 2H_{BAB}(T_1, T_2)] \cos \psi \cos^2 \phi + \frac{1}{2} \mu_A^{(1)2} \mu_B^{(1)} V_{BA}^{(3)} [H_{AAB}(T_1, T_2) + 2H_{ABA}(T_1, T_2)] \cos^2 \psi \cos \phi. \tag{51}
\end{aligned}$$

We note that if a sample is isotropic, the second-order response function vanishes by symmetry.<sup>45</sup> We perform a Fourier transformation of  $R^{(2)}(T_1, T_2)$  and obtain the second-order spectral density,

$$I^{(2)}(\omega_1, \omega_2) \equiv - \int_0^\infty \int_0^\infty e^{i\omega_1 T_1} e^{i\omega_2 T_2} R^{(2)}(T_1, T_2) dT_1 dT_2. \tag{52}$$

Its explicit form is too complicated to write down in this paper, and we will only show the graphical results of a representative example in Sec. VI.

## B. The third-order spectroscopy

Equation (38) with Eqs. (20)–(22) leads to the third-order dipole moment of molecule  $S$  as

$$\begin{aligned}
\mu_S^{\text{tot}(3)}(t) = & \mu_S^{(1)} q_S^{(3)}(t) \cos \theta_S + \frac{\mu_S^{(3)}}{6} q_S^{(1)3}(t) \cos \theta_S + T_{AB} \alpha_S^{(1)} \mu_{S'}^p q_S^{(3)}(t) + \frac{T_{AB}}{6} \alpha_S^{(3)} \mu_{S'}^p q_S^{(1)3}(t) + T_{AB} \alpha_S^{(0)} \mu_{S'}^{(1)} q_{S'}^{(3)}(t) \\
& + \frac{T_{AB}}{6} \alpha_S^{(0)} \mu_{S'}^{(3)} q_{S'}^{(1)3}(t) + T_{AB} \alpha_S^{(1)} \mu_{S'}^{(1)} q_{S'}^{(1)}(t) q_{S'}^{(2)}(t) + \frac{T_{AB}}{2} \alpha_S^{(1)} \mu_{S'}^{(2)} q_{S'}^{(1)}(t) q_{S'}^{(1)2}(t) + T_{AB} \alpha_S^{(1)} \mu_{S'}^{(1)} q_{S'}^{(2)}(t) q_{S'}^{(1)}(t) \\
& + \frac{T_{AB}}{2} \alpha_S^{(2)} \mu_{S'}^{(1)} q_{S'}^{(1)2}(t) q_{S'}^{(1)}(t). \tag{53}
\end{aligned}$$

Substituting Eqs. (29) and (31) and the explicit third-order solution  $q_S^{(3)}(t)$  written in our Technical Note<sup>42</sup> for the above equation, we obtain  $\mu_S^{\text{tot}(3)}(t)$  as presented in Appendix D. For the third-order spectroscopy, we define the external electric field  $E_{\text{ex}}(t)$  as

$$E_{\text{ex}}(t) = E_0 \delta(t) + E_0 \delta(t - T_1) + E_0 \delta(t - T_1 - T_2). \tag{54}$$

(See Fig. 2.) The insertion of Eq. (54) into Eq. (D1) leads to  $\mu_S^{\text{tot}(3)}(T_{123})$  whose full explicit form has never been obtained

in previous studies.<sup>24,25</sup> It is given in our Technical Note.<sup>42</sup> Note that we put  $T_{123} \equiv T_1 + T_2 + T_3$ . From Eq. (37) and the explicit form of  $\mu_S^{\text{tot}(3)}(T_{123})$  derived in this paper, we can obtain the third-order response function defined by  $P^{(3)}(T_{123}) \equiv n_0 E_0^3 R^{(3)}(T_1, T_2, T_3)$  as

$$\begin{aligned}
R^{(3)}(T_1, T_2, T_3) = & N^{(3)}(T_1, T_2, T_3) + T^{(3)}(T_1, T_2, T_3) \\
& + D^{(3)}(T_1, T_2, T_3) + A^{(3)}(T_1, T_2, T_3), \tag{55}
\end{aligned}$$

where each contribution is explicitly given in Appendix E.



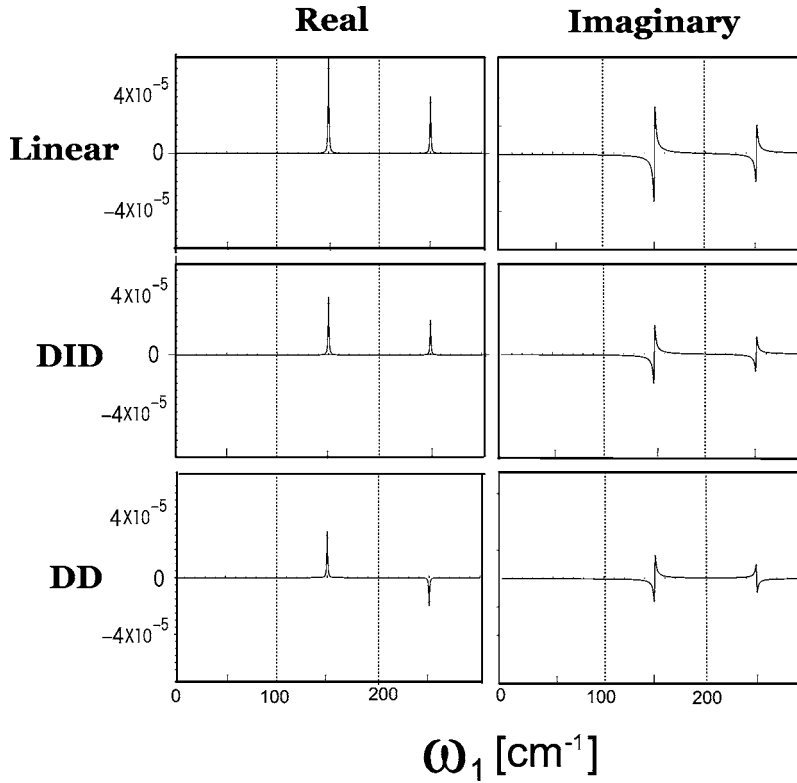


FIG. 3. The linear IR spectral density  $I^{(1)}(\omega_1)$  in Eq. (B1). The unit of vertical axis is  $q^2/4\pi^2c^2M$  with the speed of light  $c$  (cm/s). The upper, middle, and lower figures correspond to the contributions from the linear dipole coefficient, the DID interaction, and the DD interaction in  $I^{(1)}(\omega_1)$ , respectively. The left three figures show real parts of the linear spectral density,  $\text{Re}[I^{(1)}(\omega_1)]$ , while the right ones show imaginary parts of it,  $\text{Im}[I^{(1)}(\omega_1)]$ .

Even if a sample is isotropic, the third-order response function never vanishes, and it finally becomes the leading-order term of the nonlinear spectroscopy. We perform the following Fourier transformations and derive the third-order spectral densities which are observable in the experiments:

$$I_1^{(3)}(T_1, \omega_2, \omega_3) \equiv - \int_0^\infty \int_0^\infty e^{i\omega_2 T_2} e^{i\omega_3 T_3} R^{(3)}(T_1, T_2, T_3) dT_2 dT_3, \quad (56)$$

$$I_2^{(3)}(\omega_1, T_2, \omega_3) \equiv - \int_0^\infty \int_0^\infty e^{i\omega_1 T_1} e^{i\omega_3 T_3} \times R^{(3)}(T_1, T_2, T_3) dT_1 dT_3, \quad (57)$$

and

$$I_3^{(3)}(\omega_1, \omega_2, T_3) \equiv - \int_0^\infty \int_0^\infty e^{i\omega_1 T_1} e^{i\omega_2 T_2} \times R^{(3)}(T_1, T_2, T_3) dT_1 dT_2. \quad (58)$$

Explicit forms of the above are so complicated that we only show those results of a representative example graphically in the next section.

## VI. REPRESENTATIVE CALCULATIONS

We shall now demonstrate the advantage of multidimensional IR spectroscopy by plotting the representative signals using the analytical expressions derived in Secs. IV and V. We have set the mass, fundamental frequencies, and dissipation constants of vibration modes  $A$  and  $B$  as  $m_A = m_B = 1[M]$ ,  $\Omega_A = 179.5 \text{ cm}^{-1}$  and  $\Omega_B = 268.8 \text{ cm}^{-1}$ , and  $\gamma_A = \gamma_B = 1 \text{ cm}^{-1}$ , respectively, where  $M$  denotes the mass of a pro-

ton. In comparison with the previous studies,<sup>34,44,46,47</sup> we set the values of the coefficients as follows. The permanent and expanded dipole coefficients are given as  $\mu_A^p = \mu_B^p = 1[qa_0]$ ,  $\mu_A^{(1)} = \mu_B^{(1)} = 0.1[q]$ , and  $\mu_A^{(2)} = \mu_B^{(2)} = 0.01[qa_0^{-1}]$ , while the expanded polarization coefficients are set as  $\alpha_A^{(0)} = \alpha_B^{(0)} = 1[4\pi\epsilon_0 a_0^3]$  and  $\alpha_A^{(1)} = \alpha_B^{(1)} = 1[4\pi\epsilon_0 a_0^2]$ . Here,  $q$  and  $a_0$  indicate the charge of an electron and the Bohr radius, respectively.

### A. Linear absorption spectroscopy

First, we illustrate linear absorption spectra [Eq. (B1)] in Fig. 3. Although one can set any values to calculate a signal from our analytical expressions, we adopt  $\psi = \phi = 0$  rad for simplicity, which leads to

$$\tilde{T}_{AB} = \tilde{D}_{AB} = \frac{3\langle \cos^2 \theta_{AB} \rangle - 1}{4\pi\epsilon_0 \langle r_{AB}^3 \rangle}, \quad (59)$$

where  $\theta_{AB}$  and  $r_{AB}$  are assumed to be independently distributed. The structure constants are set as  $\langle r_{AB}^3 \rangle = 27[a_0^3]$  and  $\langle \cos^2 \theta_{AB} \rangle = 2/3$  in  $\tilde{T}_{AB}$  and  $\tilde{D}_{AB}$ .

As seen in Fig. 3, there are only two peaks which correspond to vibration modes  $A$  and  $B$ , respectively. We note that the values of the peak frequencies are clearly different from the original fundamental frequencies  $\Omega_A = 179.5 \text{ cm}^{-1}$  and  $\Omega_B = 268.8 \text{ cm}^{-1}$ , as a result of the effects of the DD interaction and dissipation. [See Eqs. (19) and (25).] It should be also emphasized that the effects of the DID interaction from  $\tilde{T}_{AB}$  and the effects of the DD interaction from  $\tilde{D}_{AB}$  are not distinguishable through linear IR spectroscopy because the effects appear at the same peak frequencies. The nonlinearity of dipole moment such as  $\mu_S^{(2)}$  does not contribute to the intensity of the linear IR spectra.

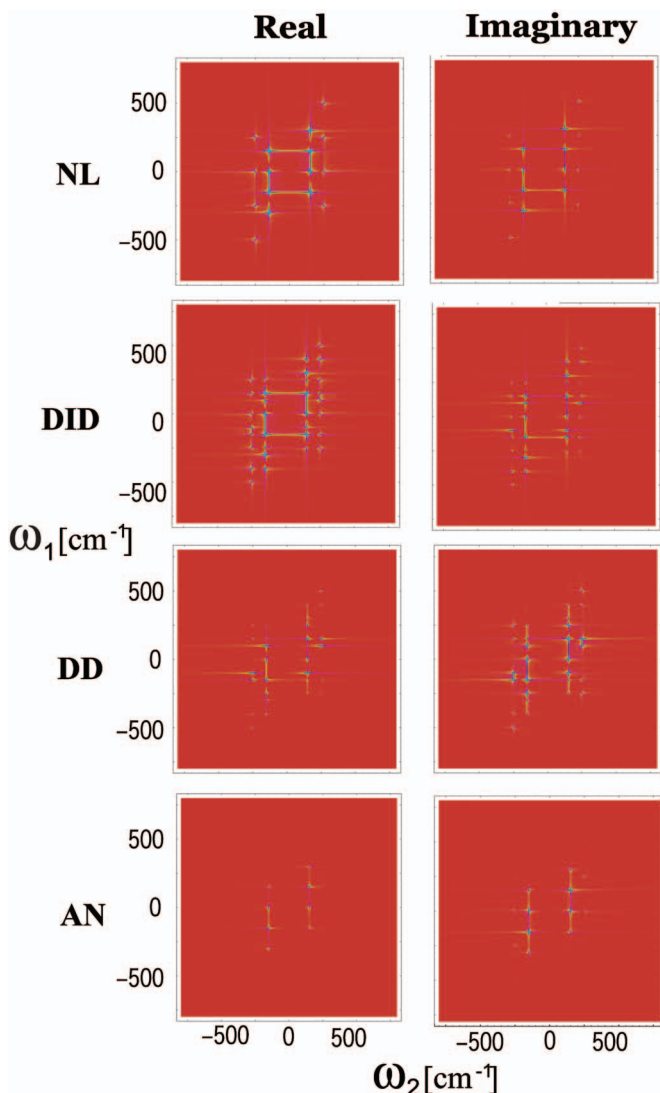


FIG. 4. (Color) Contour plots of the second-order IR spectra  $I^{(2)}(\omega_1, \omega_2)$ . The left four figures show  $\text{Re}[I^{(2)}(\omega_1, \omega_2)]$ , while the right ones show  $\text{Im}[I^{(2)}(\omega_1, \omega_2)]$ . The upper, upper-middle, lower-middle, and lower figures show the contributions from the nonlinear dipole coefficient, the DID interaction, the DD interaction, and the anharmonicity in  $I^{(2)}(\omega_1, \omega_2)$ , respectively.

## B. The second-order IR spectroscopy

In Fig. 4, we depict the second-order spectra [Eq. (52)]. We note that they disappear in isotropic samples. All the numerical coefficients have the same values as those in Sec. VI A, but the following coefficients are added here:  $V_B^{(3)} = V_B^{(3)} = 3.704 \times 10^{-5} [q^2 / 4\pi\epsilon_0 a_0^4]$ ,  $V_{AB}^{(3)} = V_{BA}^{(3)} = 0 [q^2 / 4\pi\epsilon_0 a_0^4]$ , and  $\alpha_A^{(2)} = \alpha_B^{(2)} = 0.1 [4\pi\epsilon_0 a_0]$ . Compared with linear absorption spectra, more peaks appear in the second-order IR experiments. This is because, in the second-order IR experiments, a sample interacts with the external field twice and the second-order spectra include two vibrational excitation and deexcitation processes. However, even if the second-order response function did not vanish, it would be difficult to distinguish the effects of the DD and DID interactions and the anharmonicity from each other through the second-order spectra because the peaks which are attributed to these effects usually overlap with comparable strengths.

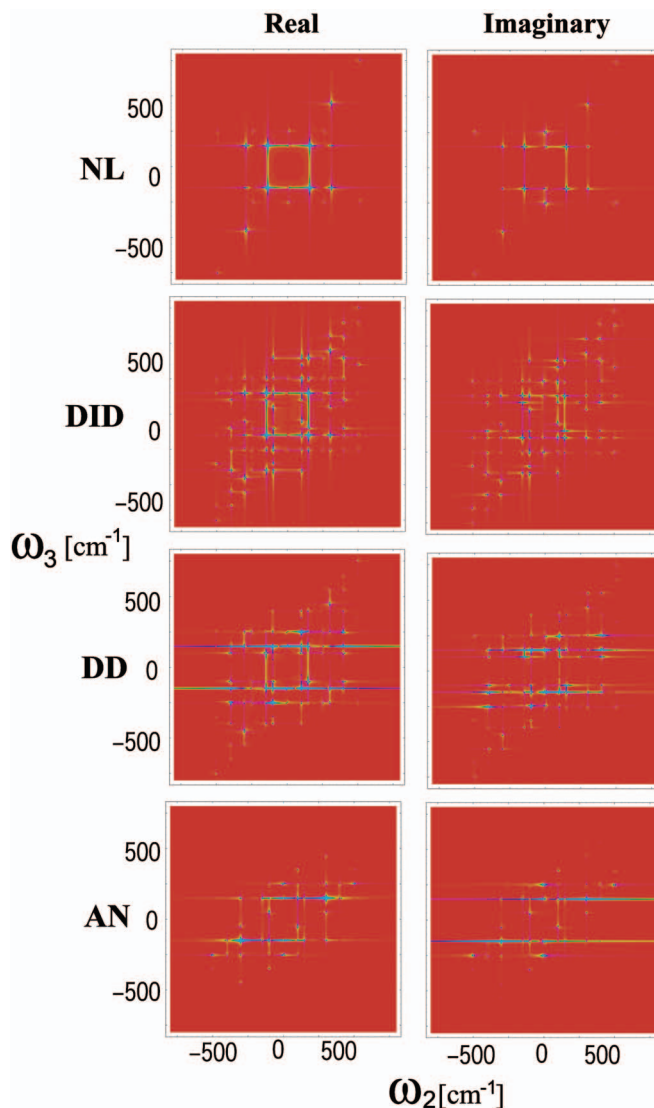


FIG. 5. (Color) Contour plots of the third-order IR spectra  $I_1^{(3)}(T_1, \omega_2, \omega_3)$  at  $T_1 = 42.4$  ps. The left four figures show  $\text{Re}[I_1^{(3)}(T_1, \omega_2, \omega_3)]$ , while the right ones show  $\text{Im}[I_1^{(3)}(T_1, \omega_2, \omega_3)]$ . The upper, upper-middle, lower-middle, and lower figures show the contributions from the nonlinearity of the dipole moment, the DID interaction, the DD interaction, and the anharmonicity, respectively.

## C. The third-order IR spectroscopy

We now present graphical results of the third-order spectra expressed by Eqs. (56)–(58). All the numerical coefficients have the same values as those in Secs. VI A and VI B, but the following coefficients are added here:  $\mu_B^{(3)} = \mu_B^{(3)} = 0.001 [qa_0^{-2}]$ ,  $\alpha_A^{(3)} = \alpha_B^{(3)} = 0.01 [4\pi\epsilon_0]$ ,  $V_B^{(4)} = V_B^{(4)} = V_{AB}^{(4)} = V_{BA}^{(4)} = 3.704 \times 10^{-6} [q^2 / 4\pi\epsilon_0 a_0^5]$ , and  $V_{AB}^{(4)} = V_{BA}^{(4)} = 0 [q^2 / 4\pi\epsilon_0 a_0^5]$ . Since we have three time variables,  $T_1$ ,  $T_2$ , and  $T_3$ , there are several ways to plot the third-order signals. Based on our analytical expressions, we have calculated the double-Fourier-transferred signals with the fixed time constants  $T_1$ ,  $T_2$ , and  $T_3$ .

We found that  $I_1^{(3)}(T_1, \omega_2, \omega_3)$  and  $I_2^{(3)}(\omega_1, T_2, \omega_3)$  have the capability to isolate the DID contribution. Figures 5 and 6 show  $I_1^{(3)}(T_1, \omega_2, \omega_3)$  at  $T_1 = 42.4$  ps and  $I_2^{(3)}(\omega_1, T_2, \omega_3)$  at  $T_2 = 0$  s, respectively. It can be seen that, although many peaks arise from three vibrational excitation and deexcitation

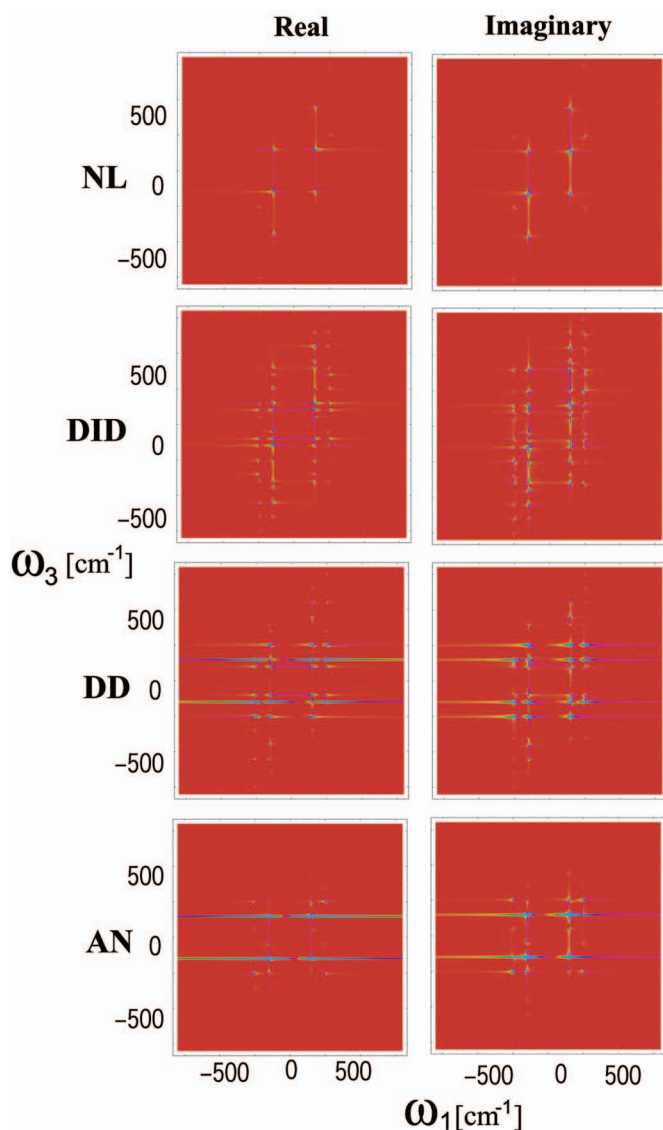


FIG. 6. (Color) The same as Fig. 5 but  $I_2^{(3)}(\omega_1, T_2, \omega_3)$  at  $T_2=0$  s, and the horizontal axis is  $\omega_1$ .

processes, the majority of them still overlap with the others even in the third-order IR measurement. There are some peaks, however, where only the DID contribution becomes dominant. This fact allows us to clearly extract the DID contribution distinguished from all the others. The corresponding magnified figures of Figs. 5 and 6 are given in Fig. 7. As Fig. 7 illustrates, some peaks dominantly reflect effects of the DID interaction. We confirmed that the peak appearing around  $(\omega_2, \omega_3)=(100, 350)$  in the upper-right figure of Fig. 7 and that around  $(\omega_1, \omega_3)=(250, 350)$  in the lower-right figure are both proportional to  $\tilde{T}_{AB}\mu_A^{(1)}\mu_B^{(1)2}(\mu_A^{(1)}\alpha_B^{(2)} + \alpha_A^{(1)}\mu_B^{(2)})$ . These peaks enable us to obtain structural information on molecules *A* and *B* because they are proportional to  $1/\langle r_{AB}^3 \rangle$  through the factor  $\tilde{T}_{AB}$ . We should note, however, that it is usually difficult to determine the absolute value of each peak, so that one can obtain only relative distances of molecules *A* and *B* at different times.<sup>27</sup>

Figures 8 and 9 show  $I_3^{(3)}(\omega_1, \omega_2, T_3)$  at  $T_3=530.5$  fs and at  $T_3=42.4$  ps. We have found that as  $T_3$  becomes large, the

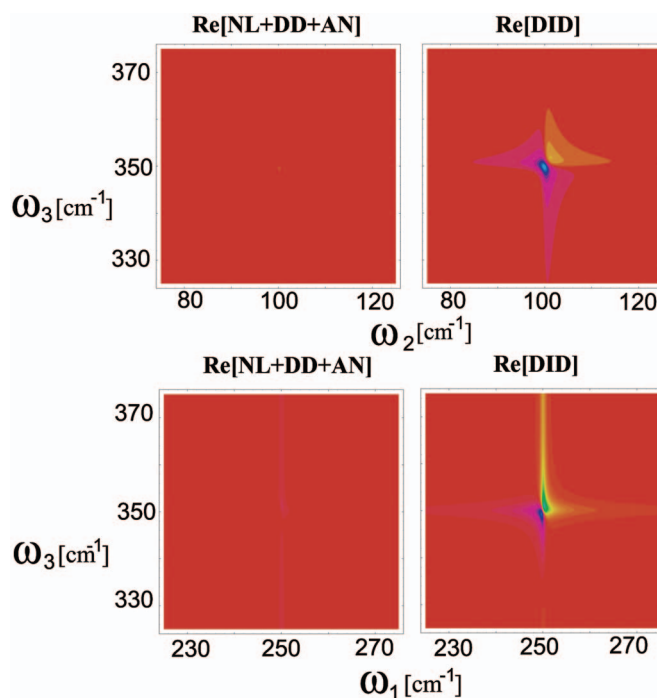


FIG. 7. (Color) Magnified views of the real part of Fig. 5 (the upper two figures) and Fig. 6 (the lower two figures). The left figures show sums of the contributions from the nonlinear dipole coefficient, the DD interaction, and the anharmonicity, while the right ones show those from the DID interaction.

contributions from the DD interaction and the anharmonicity of each vibrational mode in  $I_3^{(3)}(\omega_1, \omega_2, T_3)$  become dominant compared with the contributions from the nonlinearity of the dipole moment and the DID interaction. This fact indicates that the vibrational excitations caused by the DD interaction and the anharmonicity decay slower than those caused by the other two effects, as can be clearly seen in the third-order response functions presented in Fig. 10. The above findings enable us to extract the DD interaction and the anharmonicity independently of the third-order IR signals. The DD and anharmonic contributions in Fig. 9 are magnified and presented in Fig. 11; each peak clearly reflects the DD interaction or the anharmonicity. The physical origins of these peaks can be identified from our explicit expressions of  $I_3^{(3)}(\omega_1, \omega_2, T_3)$ . The peak appearing around  $(\omega_1, \omega_2)=(250, 400)$  in the upper-right figure is proportional to  $\tilde{D}_{AB}\mu_A^{(1)2}\mu_B^{(1)2}\mu_A^{(2)}\mu_B^{(2)}$ , while that around  $(\omega_1, \omega_2)=(150, 300)$  in the lower-right figure is proportional to  $V_A^{(4)}\mu_A^{(1)4}$ . Since  $\tilde{D}_{AB}$  is also proportional to  $1/\langle r_{AB}^3 \rangle$ , we can cross-check the information of molecular structures through the DID and DD interactions, if we measure  $I_3^{(3)}(\omega_1, \omega_2, T_3)$  and  $I_1^{(3)}(T_1, \omega_2, \omega_3)$  or  $I_2^{(3)}(\omega_1, T_2, \omega_3)$  together. Furthermore, one can specify the strength of the anharmonicity by detecting the peak intensity around  $(\omega_1, \omega_2)=(150, 300)$ . Finally, it is worth mentioning that  $I_3^{(3)}(\omega_1, \omega_2, T_3)$  derived in this paper tends to be zero with  $T_3 \rightarrow 0$ . This indicates that we can easily justify an applicability of our formula to the system which we are interested in by checking the  $T_3$  dependency of the signal. Although we could not extract the contribution from the nonlinearity of dipole *A* or *B* even through the

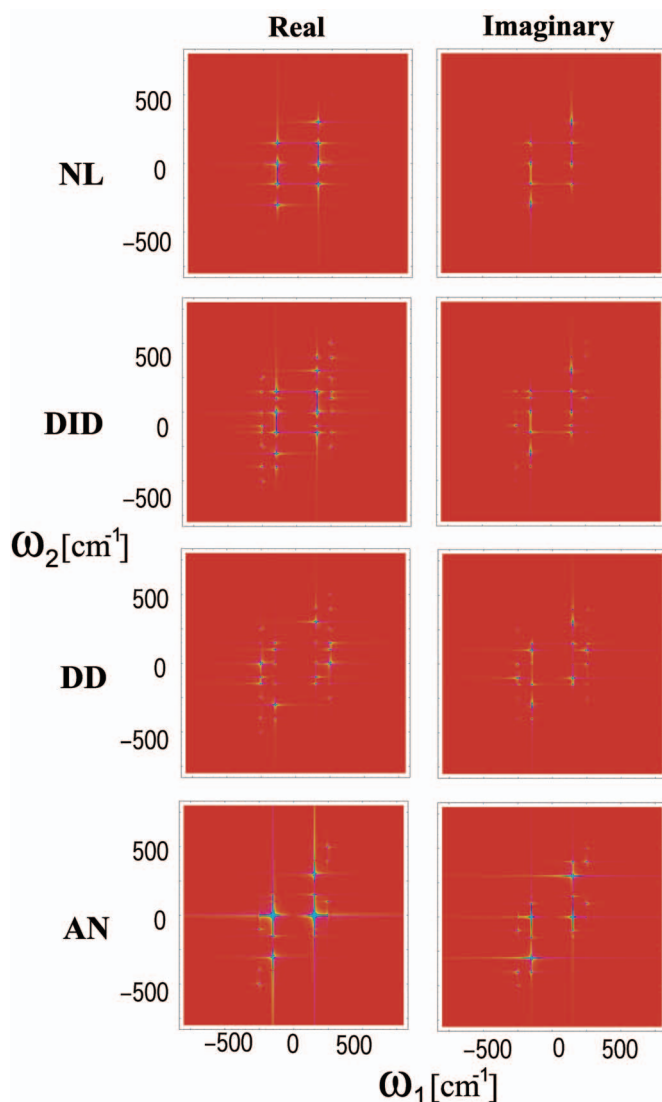


FIG. 8. (Color) The same as Fig. 5 but  $I_3^{(3)}(\omega_1, \omega_2, T_3)$  at  $T_3=530.5$  fs, and the horizontal and the vertical axes are  $\omega_2$  and  $\omega_3$ , respectively.

third-order spectra derived in this paper, it can be detected from another type of the third-order IR spectroscopy proposed by previous studies.<sup>8,25,44,48–54</sup>

## VII. SUMMARY AND DISCUSSION

We have derived analytical expressions for the first-, second-, and third-order IR spectra of two interacting dipolar modes for various space configurations. All of the essential interactions between dipoles, the DID and DD interactions, as well as the cubic and quadratic anharmonicities of vibrational potentials and the nonlinearity of dipole moments are taken into account. Our analytical calculations give each explicit contribution to the peaks in the IR spectra as the separated terms and give us their clear physical origins. We emphasize that each order of the IR signals calculated here contains all the contributions classified by each order of the Liouville paths in the vibrational-energy-level representation, and we give the results not around a specific frequency but over the whole range of frequencies. It should be noted that there is a theoretical means to separate the contributions of

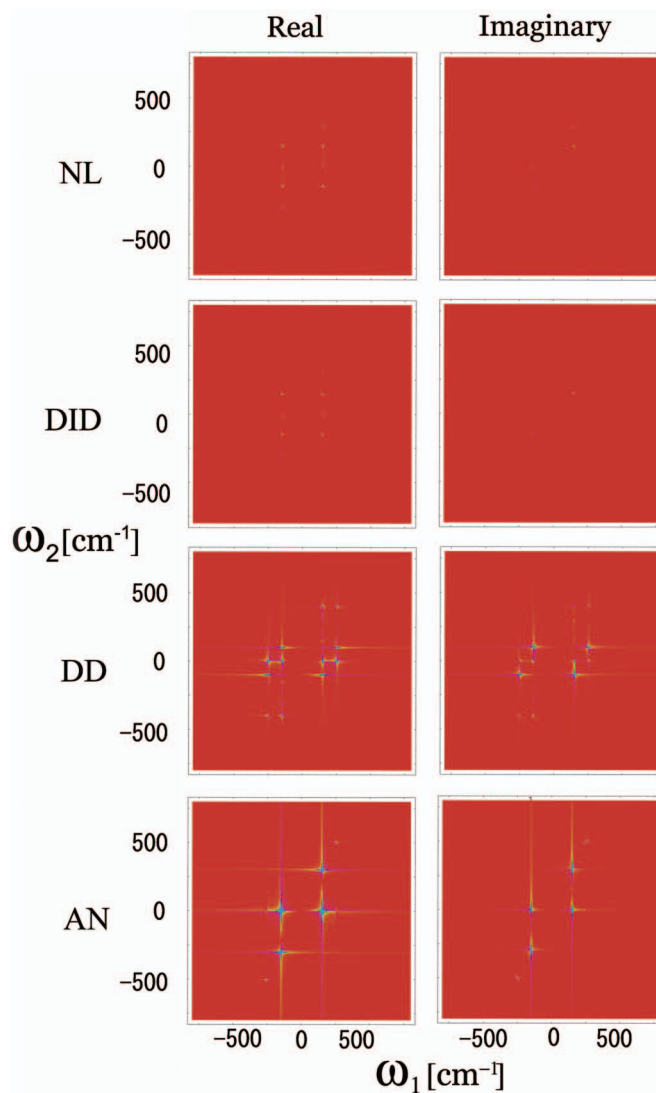


FIG. 9. (Color) The same as Fig. 8 but at  $T_3=42.4$  ps.

different Liouville paths from our expression of the signals; each path is separately detected experimentally with the phase-matching conditions.<sup>20</sup>

Our representative calculations have demonstrated the following advantage and usefulness of the third-order spectroscopy. Whereas the contributions from DID and DD interactions and the anharmonicity of the potential were comparably overlapped and could not be identified in the first- and second-order IR spectroscopies, they were distinguishable from each other through the third-order signals. Such identification is important, especially in the case when contributions from the DID and DD interactions and the anharmonicities are comparable, which often occurs as was demonstrated in our representative calculation. Even in such complex systems where each effect appears, the above findings enable us to obtain the structural information of molecules within the femtosecond range. Furthermore, since the third-order 2D signals  $I_1^{(3)}(T_1, \omega_2, \omega_3)$  and  $I_2^{(3)}(\omega_1, T_2, \omega_3)$  detect  $\tilde{T}_{AB}$ , whereas  $I_3^{(3)}(\omega_1, \omega_2, T_3)$  identifies  $\tilde{D}_{AB}$ , the structural information can be cross-checked through a comparison of the DID and DD interactions. Actually, in our calculation, we



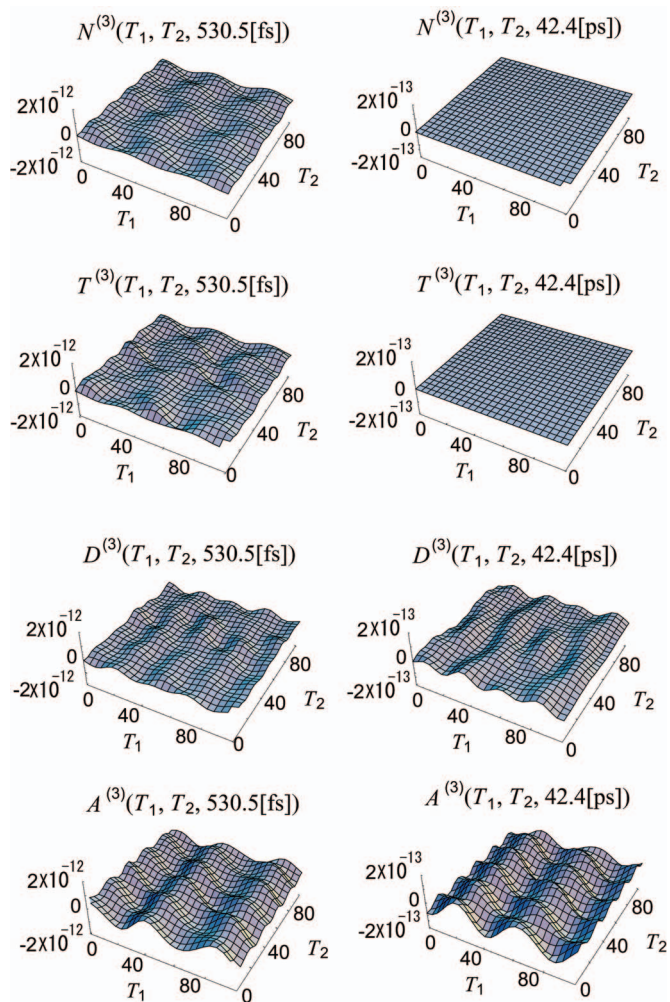


FIG. 10. (Color) The third-order response functions from the nonlinear dipole coefficient  $N^{(3)}(T_1, T_2, T_3)$  (upper), the DID interaction  $T^{(3)}(T_1, T_2, T_3)$  (middle-upper), the DD interaction  $D^{(3)}(T_1, T_2, T_3)$  (middle-lower), and the anharmonicity  $A^{(3)}(T_1, T_2, T_3)$  (lower). The unit of both axes  $T_1$  and  $T_2$  is  $1/2\pi c[\text{s}]$ . The unit of vertical axis is  $q^4/8\pi^2 c^3 M^3 a_0^2$ . We set  $T_3=530.5$  fs in the left figures and  $T_3=42.4$  ps in the right ones.

have presented some explicit peak intensities which reflect dominantly the DID or DD interaction or the anharmonicity.

In this paper, we have adopted the molecular coordinate picture introducing many contributions such as the vibration relaxation, the interacting dipolar potentials, and the anharmonicities with the various dipolar material parameters and space configurations. Thus, our analytical expressions contain many parameters. Compared with the vibrational-energy-level picture which is defined by eigenenergy levels with possible optical and bath-induced transition elements between them, the molecular coordinate picture is intuitive and makes it easy to settle the parameters. In fact, while we have demonstrated the IR spectra only for one parameter set in Sec. VI, there is no difficulty in changing any parameter according to the system being examined. For example, we could easily check the effects of dissipation by increasing the damping constant as  $\gamma_S=10$   $\text{cm}^{-1}$ , and we have confirmed the broadening and deviation of spectral peaks following Eq. (19).

Owing to the analytically explicit expressions, we have

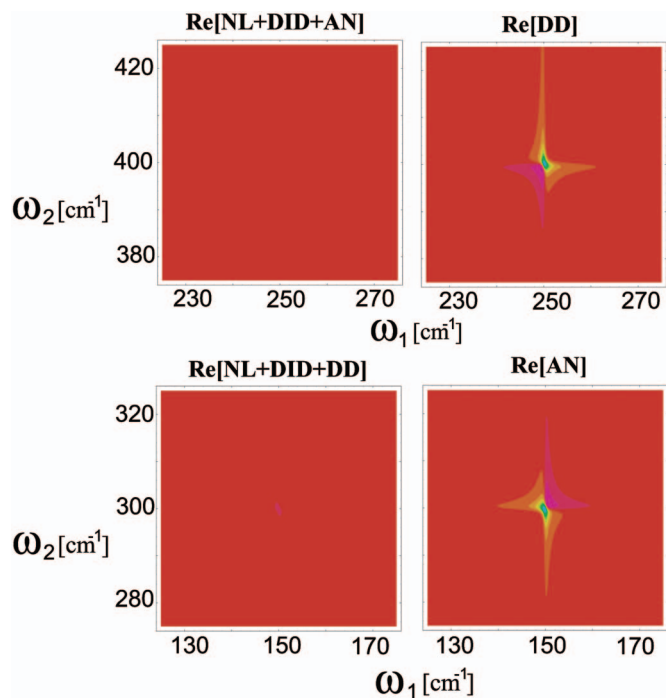


FIG. 11. (Color) Magnified views of the real part of Fig. 9. The upper-left figure represents the effects from the nonlinear dipole coefficient, the DID interaction, and the anharmonicity, while the upper-right one represents the effect of the DD interaction. The lower-left figure shows a sum of the contributions from the nonlinear dipole coefficient, the DID interaction, and the DD interaction, while the lower-right one shows the contribution from the anharmonicity.

developed a handy analysis program for IR experiments and simulations. This program can be downloaded from our website upon users' request.<sup>42</sup> We emphasize that the above program can be applied to any pairwise interacting molecules. Possible targets are C=O and N-H bonds of an  $\alpha$  helix and C=O bonds of a  $\beta$  sheet in proteins. The structural information within ultrafast time scales of DNA transition can be also examined by our program, since DNA includes dipolar interactions between adenine-guanine or cytosine-thymine molecule pairs. It may be interesting to apply our program to dimeric systems of peptides, e.g., *N*-methylacetamide or other biomolecules.

Because our formalization is based on a classical picture of molecular vibrations, there are some limitations to its applicability. For example, if the anharmonicity of vibrational potentials is strong and the fundamental frequencies of vibration modes are much higher than the thermal energy, the quantum effects become essential.<sup>52,55,56</sup> Our analytical results should not be applied to such cases. However, our results should be examined for moderately high-frequency modes such as C=O and N-H bond interactions. It is also important to check any differences or similarities between our results and those based on the vibrational-energy-level models.<sup>37-39</sup> We took into account only the dissipation by damping constants and did not consider any thermal fluctuations. If we introduce a Langevin random force which is related to the damping term through the fluctuation dissipation theorem to the equations of vibrational motion (1) and (2), we could account for temperature effects. Note that, in order to include the spectral distribution of the thermal noise,



we have to adopt not the Langevin equation but the generalized Langevin equation which is characterized by a time-dependent damping term, that is, a memory term. In addition, sorts of system-bath coupling affect the temperature dependency, while we consider the temperature-independent case which corresponds to the bilinear system-bath coupling systems.<sup>53</sup> This fact suggests that we should pay attention to the effects of the surrounding solution or connecting main bonds. The effects of the vibrational dephasing are not included in the present paper. Such phenomena are caused by the nonlinear coupling between the system and bath modes and play an important role in both classical and quantum spectroscopies: In the coordinate representation, the quadratic-linear system-bath coupling term reflects the vibrational dephasing effect.<sup>9,22,57</sup>

Although we have studied only two interacting dipoles, so long as only pairwise interactions are involved, we can easily extend the present results to a many-mode system by decomposing the many-body interactions into the pairwise ones and by overlapping the signals with each other. However, if a sample consists of numerous pairs of interacting dipoles, the spectral profile is affected by their statistical distributions. A sample of uniformly distributed dipole pairs results in  $\tilde{T}_{AB} = \tilde{D}_{AB} = 0$  with  $\psi = \phi = 0$  rad from  $\langle \cos^2 \theta_{AB} \rangle = 1/3$ , while that of dipole pairs whose distribution is described by a canonical distribution with the temperature  $T_g$  leads to  $\langle \cos^2 \theta_{AB} \rangle \sim 1/T_g \langle r_{AB}^3 \rangle$  within a high-temperature approximation. We should also mention that, in general, huge

and high-molecular-weight reacting molecules cannot be quickly adjusted to their environmental temperature at each moment, and the distributions of dipole pairs in reacting biomolecules are difficult to determine. The above problem might be solved when a single molecule spectroscopy is practicable, or when molecules in a thin sample can be placed in order.

In conclusion, we have derived analytical expressions for linear-, second-, and third-order IR spectra in terms of the contributions from the nonlinearity of the dipole moment and the polarizability, the DID and DD interactions, the anharmonicity of vibrational potentials, and the anharmonic mode-mode coupling. Our formula will provide a powerful tool for studying molecular interactions and structures, although there is room for improvement in the theory.

## ACKNOWLEDGMENTS

We would like to express our sincere thanks to K. Okumura, S. Saito, H. Torii, and R. J. Dwayne Miller for their fruitful discussions, and M. Maroncelli and Y. Ueno for reviewing our manuscripts. This research is partially supported by Grant-in-Aids for Scientific Research from Japan Society for the Promotion of Science, Grants No. 17740278 and No. A15205005.

## APPENDIX A: DEFINITION OF $G_{AB}(T_1)$

We define  $G_{AB}(T_1)$  as

$$G_{AB}(T_1) \equiv \int d\tau D_{S'}(T_1 - \tau) D_S(\tau) \quad (\text{A1})$$

$$= \int_0^{T_1} d\tau e^{-(\gamma_S \tau^2) - (\gamma_{S'}(T_1 - \tau)^2)} \frac{\sin \xi_S \tau \sin \xi_{S'}(T_1 - \tau)}{m_S \xi_S m_{S'} \xi_{S'}} \quad (\text{A2})$$

$$= \frac{4[4(\gamma_S - \gamma_{S'})\xi_S(D'_S(T_1)/m_{S'}) + \{(\gamma_S - \gamma_{S'})^2 - 4(\xi_S^2 - \xi_{S'}^2)\}(D_S(T_1)/m_{S'})]}{\{(\gamma_S - \gamma_{S'})^2 + 4\xi_S^2\}^2 + 8\{(\gamma_S - \gamma_{S'})^2 - 4\xi_S^2\}\xi_{S'}^2 + 16\xi_{S'}^4} + \frac{4[4(\gamma_{S'} - \gamma_S)\xi_{S'}(D'_{S'}(T_1)/m_S) + \{(\gamma_S - \gamma_{S'})^2 - 4(\xi_{S'}^2 - \xi_S^2)\}(D_{S'}(T_1)/m_S)]}{\{(\gamma_S - \gamma_{S'})^2 + 4\xi_{S'}^2\}^2 + 8\{(\gamma_S - \gamma_{S'})^2 - 4\xi_{S'}^2\}\xi_S^2 + 16\xi_S^4}, \quad (\text{A3})$$

with

$$D'_S(\tau) \equiv \Theta(\tau) \frac{e^{-\gamma_S \tau^2}}{m_S \xi_S} \cos \xi_S \tau. \quad (\text{A4})$$

Note that  $G_{AB} = G_{BA}$ .

## APPENDIX B: DEFINITION OF $I^{(1)}(\omega_1)$

The first-order spectral density results in

$$\begin{aligned}
I^{(1)}(\omega_1) = & \mu_A^{(1)2} L_A(\omega_1) \cos^2 \psi + \mu_B^{(1)2} L_B(\omega_1) \cos^2 \phi + \frac{3}{2} T_{AB} \mu_A^{(1)} \Phi_{AB}^{(1,0)} L_A(\omega_1) \cos \psi + \frac{3}{2} T_{AB} \mu_B^{(1)} \Phi_{AB}^{(0,1)} L_B(\omega_1) \cos \phi \\
& + 8 D_{AB} \mu_A^{(1)2} \mu_B^{(1)2} \frac{4(\gamma_A - \gamma_B) \xi_A L'_A(\omega_1) + \{(\gamma_A - \gamma_B)^2 - 4(\xi_A^2 - \xi_B^2)\} L_A(\omega_1)}{m_B [\{(\gamma_A - \gamma_B)^2 + 4\xi_A^2\}^2 + 8\{(\gamma_A - \gamma_B)^2 - 4\xi_A^2\} \xi_B^2 + 16\xi_B^4]} \cos \psi \cos \phi \\
& + 8 D_{AB} \mu_A^{(1)2} \mu_B^{(1)2} \frac{4(\gamma_B - \gamma_A) \xi_B L'_B(\omega_1) + \{(\gamma_A - \gamma_B)^2 - 4(\xi_B^2 - \xi_A^2)\} L_B(\omega_1)}{m_A [\{(\gamma_A - \gamma_B)^2 + 4\xi_A^2\}^2 + 8\{(\gamma_A - \gamma_B)^2 - 4\xi_A^2\} \xi_B^2 + 16\xi_B^4]} \cos \psi \cos \phi, \tag{B1}
\end{aligned}$$

with

$$L_S(\omega_1) \equiv -i \int_0^\infty e^{i\omega_1 T_1} D_S(T_1) dT_1 \tag{B2}$$

$$= \frac{16\gamma_S \omega_1}{m_S \{\gamma_S^4 + 16(\omega_1^2 - \xi_S^2)^2 + 8\gamma_S^2(\omega_1^2 + \xi_S^2)\}} \tag{B3}$$

and

$$L'_S(\omega_1) \equiv -i \int_0^\infty e^{i\omega_1 T_1} D'_S(T_1) dT_1 \tag{B4}$$

$$= \frac{4\omega_1(\gamma_S^2 + 4\omega_1^2 - 4\xi_S^2)}{m_S \xi_S \{\gamma_S^4 + 16(\omega_1^2 - \xi_S^2)^2 + 8\gamma_S^2(\omega_1^2 + \xi_S^2)\}}. \tag{B5}$$

### APPENDIX C: EXPLICIT FORM OF THE SECOND-ORDER DIPOLE MOMENT

The second-order dipole moment is obtained as

$$\begin{aligned}
\mu_S^{\text{tot}(2)}(t) = & \mu_S^{(1)2} \mu_S^{(2)} A_{SS}(t) \cos^3 \theta_S + \frac{1}{2} \mu_S^{(1)2} \mu_S^{(2)} G_{SS}(t) \cos^3 \theta_S + \frac{T_{AB}}{2} \mu_S^{(1)} \{\Phi_{SS}^{(1,2)} \mu_{S'}^p + 2\alpha_{S'}^{(0)} \mu_S^{(1)} \mu_S^{(2)}\} A_{SS}(t) \cos^2 \theta_S \\
& + \frac{T_{AB}}{2} \mu_S^{(1)} \mu_{S'}^{(1)} \Phi_{SS'}^{(1,1)} A_{S'S}(t) \cos \theta_S \cos \theta_{S'} + \frac{T_{AB}}{2} \mu_S^{(1)} \mu_S^{(2)} \Phi_{SS'}^{(1,0)} G_{SS}(t) \cos^2 \theta_S + T_{AB} \alpha_S^{(1)} \mu_S^{(1)} \mu_S^{(2)} \mu_{S'}^p A_{SS}(t) \cos^2 \theta_S \\
& + T_{AB} \alpha_S^{(0)} \mu_{S'}^{(1)2} \mu_S^{(2)} A_{S'S'}(t) \cos^2 \theta_{S'} + \frac{T_{AB}}{2} \mu_S^{(1)2} \alpha_S^{(2)} \mu_{S'}^p G_{SS}(t) \cos^2 \theta_S + \frac{T_{AB}}{2} \alpha_S^{(0)} \mu_{S'}^{(1)2} \mu_S^{(2)} G_{S'S'}(t) \cos^2 \theta_{S'} \\
& + T_{AB} \alpha_S^{(1)} \mu_S^{(1)} \mu_{S'}^{(1)2} G_{S'S}(t) \cos \theta_S \cos \theta_{S'} + D_{AB} \mu_S^{(1)2} \mu_S^{(2)} \mu_{S'}^{(1)2} B_{S'SS}(t) \cos^2 \theta_S \cos \theta_{S'} \\
& + \frac{D_{AB}}{2} \{\mu_S^{(1)2} \mu_{S'}^{(1)2} \mu_S^{(2)} C_{S'S'S}(t) \cos \theta_S \cos^2 \theta_{S'} + 2\mu_S^{(1)2} \mu_S^{(2)} \mu_{S'}^{(1)2} C_{S'SS}(t) \cos^2 \theta_S \cos \theta_{S'}\} \\
& + D_{AB} \mu_S^{(1)2} \mu_{S'}^{(1)2} \mu_S^{(2)} F_{S'S'S}(t) \cos \theta_S \cos^2 \theta_{S'} + D_{AB} \mu_S^{(1)2} \mu_S^{(2)} \mu_{S'}^{(1)2} J_{SS'S}(t) \cos^2 \theta_S \cos \theta_{S'} + \frac{1}{2} \mu_S^{(1)} \\
& \times [\mu_S^{(1)2} V_S^{(3)} C_{SSS}(t) \cos^2 \theta_S + \mu_{S'}^{(1)2} V_{SS'}^{(3)} C_{S'S'S}(t) \cos^2 \theta_{S'} + \mu_S^{(1)} \mu_{S'}^{(1)} V_{S'S}^{(3)} C_{S'SS}(t) \cos \theta_S \cos \theta_{S'}] \cos \theta_S, \tag{C1}
\end{aligned}$$

where we introduced the following expressions:

$$G_{S'S}(t) \equiv \int d\tau \int d\tau' E_{\text{ex}}(t - \tau) E_{\text{ex}}(t - \tau') D_{S'}(\tau') D_S(\tau) \tag{C2}$$

and

$$J_{S''S'S}(t) \equiv \int d\tau \int d\tau' \int d\tau'' E_{\text{ex}}(t-\tau'') E_{\text{ex}}(t-\tau-\tau') D_{S''}(\tau'') D_{S'}(\tau') D_S(\tau). \quad (\text{C3})$$

Using the electric field (46), this results in

$$\begin{aligned} \mu_S^{\text{tot}(2)}(T_{12}) = E_0^2 \left[ \mu_S^{(1)2} \mu_S^{(2)} \{D_S(T_1) D_S(T_2) + D_S(T_{12}) D_S(T_2)\} \cos^3 \theta_S + \frac{T_{AB}}{2} \mu_S^{(1)} (2\mu_S^{(2)} \Phi_{SS'}^{(1,0)} + \mu_{S'}^p \Phi_{SS'}^{(1,2)}) D_S(T_1) D_S(T_2) \cos^2 \theta_S \right. \\ + T_{AB} \mu_S^{(1)} \{ \Phi_{SS'}^{(1,2)} \mu_{S'}^p + \alpha_{S'}^{(0)} \mu_S^{(1)} \mu_S^{(2)} \} D_S(T_{12}) D_S(T_2) \cos^2 \theta_S + T_{AB} \alpha_S^{(0)} \mu_S^{(1)2} \mu_{S'}^{(2)} \{ D_S(T_1) D_S(T_2) \\ + D_S(T_{12}) D_S(T_2) \} \cos^2 \theta_{S'} + \frac{T_{AB}}{2} \mu_S^{(1)} \mu_{S'}^{(1)} \{ \Phi_{SS'}^{(1,1)} D_{S'}(T_1) D_S(T_2) + 2\alpha_S^{(1)} \mu_S^{(1)} D_S(T_{12}) D_{S'}(T_2) \\ + 2\alpha_S^{(1)} \mu_S^{(1)} D_{S'}(T_{12}) D_S(T_2) \} \cos \theta_S \cos \theta_{S'} + \frac{D_{AB}}{2} \mu_S^{(1)2} \mu_{S'}^{(1)2} \mu_{S'}^{(2)} \{ 2D_{S'}(T_1) G_{AB}(T_2) \\ + H_{S'S'S}(T_1, T_2) \} \cos \theta_S \cos^2 \theta_{S'} + D_{AB} \mu_S^{(1)2} \mu_S^{(2)} \mu_{S'}^{(1)2} \{ G_{AB}(T_1) D_S(T_2) + G_{AB}(T_{12}) D_S(T_2) + G_{AB}(T_2) D_S(T_{12}) \\ + H_{SS'S}(T_1, T_2) \} \cos^2 \theta_S \cos \theta_{S'} + \frac{1}{2} \mu_S^{(1)} \{ \mu_S^{(1)2} V_{SS'}^{(3)} H_{SSS}(T_1, T_2) \cos^2 \theta_S + \mu_{S'}^{(1)2} V_{SS'}^{(3)} H_{S'S'S}(T_1, T_2) \cos^2 \theta_{S'} \\ \left. + 2\mu_S^{(1)} \mu_{S'}^{(1)} V_{S'S'}^{(3)} H_{SS'S}(T_1, T_2) \cos \theta_S \cos \theta_{S'} \} \cos \theta_S \right]. \quad (\text{C4}) \end{aligned}$$

Here, we have introduced

$$\begin{aligned} H_{S'S'S}(T_1, T_2) \equiv \int d\tau \int d\tau' \int d\tau'' E_{\text{ex}}(t-\tau-\tau') E_{\text{ex}}(t-\tau-\tau'') D_{S'}(\tau') D_{S''}(\tau'') D_S(\tau) = \int d\tau \{ D_{S'}(T_{12}-\tau) D_{S''}(T_2-\tau) \\ + D_{S'}(T_2-\tau) D_{S''}(T_{12}-\tau) \} D_S(\tau), \quad (\text{C5}) \end{aligned}$$

whose explicit expressions are given in our web page.<sup>42</sup> Note that  $H_{S'S'S}(T_1, T_2) = H_{S''S'S}(T_1, T_2)$ .

#### APPENDIX D: EXPLICIT FORM OF THE THIRD-ORDER DIPOLE MOMENT

The third-order dipole moment is derived as

$$\begin{aligned} \mu_S^{\text{tot}(3)}(t) = \mu_S^{(1)2} \mu_S^{(2)2} K_{SSS}(t) \cos^4 \theta_S + \frac{1}{2} \mu_S^{(1)3} \mu_S^{(3)} M_{SSS}(t) \cos^4 \theta_S + \frac{\mu_S^{(1)3} \mu_S^{(3)}}{6} O_{SSS}(t) \cos^4 \theta_S + \frac{T_{AB}}{2} K_{SSS}(t) \mu_S^{(1)} \mu_S^{(2)} (2\mu_S^{(1)} \Phi_{SS'}^{(2,0)} \\ + \mu_S^{(2)} \Phi_{SS'}^{(1,0)}) \cos^3 \theta_S + \frac{T_{AB}}{2} \Phi_{SS'}^{(1,1)} \mu_S^{(1)} \mu_{S'}^{(1)} [\mu_S^{(2)} K_{S'SS}(t) \cos^2 \theta_S \cos \theta_{S'} + \mu_S^{(2)} K_{S'S'S}(t) \cos \theta_S \cos^2 \theta_{S'}] + \frac{T_{AB}}{4} \mu_S^{(1)} \mu_{S'}^{(1)} \\ \times [\mu_{S'}^{(1)} \Phi_{SS'}^{(1,2)} M_{S'S'S}(t) \cos \theta_S \cos^2 \theta_{S'} + 2\mu_S^{(1)} \Phi_{SS'}^{(2,1)} M_{S'SS}(t) \cos^2 \theta_S \cos \theta_{S'}] + \frac{T_{AB}}{2} \mu_S^{(1)2} \mu_S^{(3)} \Phi_{SS'}^{(1,0)} M_{SSS}(t) \cos^3 \theta_S \\ + \frac{T_{AB}}{4} \mu_S^{(1)3} \Phi_{SS'}^{(3,0)} M_{SSS}(t) \cos^3 \theta_S + \frac{T_{AB}}{4} \mu_S^{(1)2} \mu_S^{(3)} \Phi_{SS'}^{(1,0)} O_{SSS}(t) \cos^3 \theta_S + T_{AB} \alpha_S^{(1)} \mu_S^{(1)} \mu_S^{(2)2} \mu_{S'}^p K_{SSS}(t) \cos^3 \theta_S \\ + \frac{T_{AB}}{2} \alpha_S^{(1)} \mu_S^{(1)2} \mu_S^{(3)} \mu_{S'}^p M_{SSS}(t) \cos^3 \theta_S + \frac{T_{AB}}{6} \mu_S^{(1)3} \alpha_S^{(3)} \mu_{S'}^p O_{SSS}(t) \cos^3 \theta_S + T_{AB} \alpha_S^{(0)} \mu_S^{(1)2} \mu_S^{(2)2} K_{S'S'S}(t) \cos^3 \theta_{S'} \\ + \frac{T_{AB}}{2} \alpha_S^{(0)} \mu_S^{(1)3} \mu_{S'}^{(3)} M_{S'S'S}(t) \cos^3 \theta_{S'} + \frac{T_{AB}}{6} \alpha_S^{(0)} \mu_S^{(1)3} \mu_{S'}^{(3)} O_{S'S'S}(t) \cos^3 \theta_{S'} \\ + T_{AB} \alpha_S^{(1)} \mu_S^{(1)} \mu_{S'}^{(1)2} \mu_{S'}^{(2)} W_{S'S'S}(t) \cos \theta_S \cos^2 \theta_{S'} + \frac{T_{AB}}{2} \alpha_S^{(1)} \mu_S^{(1)} \mu_{S'}^{(1)2} \mu_{S'}^{(2)} O_{SS'S}(t) \cos \theta_S \cos^2 \theta_{S'} \\ + T_{AB} \alpha_S^{(1)} \mu_S^{(1)} \mu_S^{(2)} \mu_{S'}^{(1)2} W_{SSS}(t) \cos^2 \theta_S \cos \theta_{S'} + \frac{T_{AB}}{2} \mu_S^{(1)2} \alpha_S^{(2)} \mu_{S'}^{(1)2} O_{S'SS}(t) \cos^2 \theta_S \cos \theta_{S'} + \dots \\ + D_{AB} \mu_S^{(1)2} \mu_S^{(2)2} \mu_{S'}^{(1)2} X_{S'SSS}(t; \tau, \tau + \tau', \tau + \tau' + \tau'' + \tau''') \cos^3 \theta_S \cos \theta_{S'} + \frac{D_{AB}}{2} [\mu_S^{(1)2} \mu_S^{(2)} \mu_{S'}^{(1)2} \mu_{S'}^{(2)} X_{S'S'S}(t; \tau, \tau \\ + \tau' + \tau'', \tau + \tau' + \tau'' + \tau''') \cos^2 \theta_S \cos^2 \theta_{S'} + 2\mu_S^{(1)2} \mu_S^{(2)2} \mu_{S'}^{(1)2} X_{S'SSS}(t; \tau, \tau + \tau' + \tau'', \tau + \tau' + \tau''') \cos^3 \theta_S \cos \theta_{S'}] \end{aligned}$$

$$\begin{aligned}
& + D_{AB}\mu_S^{(1)2}\mu_S^{(2)}\mu_{S'}^{(1)2}\mu_{S'}^{(2)}X_{S'S'SS}(t;\tau,\tau+\tau'+\tau'',\tau+\tau'+\tau''+\tau''')\cos^2\theta_S\cos^2\theta_{S'} \\
& + D_{AB}\mu_S^{(1)3}\mu_S^{(3)}\mu_{S'}^{(1)2}X_{SSS'S}(t;\tau,\tau+\tau''',\tau+\tau'+\tau'')\cos^3\theta_S\cos\theta_{S'} + D_{AB}\mu_S^{(1)2}\mu_S^{(2)}\mu_{S'}^{(1)2}[\mu_S^{(2)}X_{SSS'S}(t;\tau+\tau',\tau \\
& + \tau'',\tau+\tau'+\tau''')\cos^3\theta_S\cos\theta_{S'} + \mu_{S'}^{(2)}X_{S'S'SS}(t;\tau+\tau',\tau+\tau'',\tau+\tau'+\tau''')\cos^2\theta_S\cos^2\theta_{S'}] \\
& + \frac{D_{AB}}{2}\mu_S^{(1)2}\mu_S^{(2)}\mu_{S'}^{(1)2}\mu_{S'}^{(2)}X_{SS'S'S}(t;\tau+\tau',\tau+\tau'',\tau+\tau''')\cos^2\theta_S\cos^2\theta_{S'} + D_{AB}\mu_S^{(1)2}\mu_{S'}^{(1)2}\mu_{S'}^{(2)2}X_{S'S'S'S}(t;\tau+\tau',\tau \\
& + \tau'+\tau'',\tau+\tau'+\tau'+\tau''')\cos\theta_S\cos^3\theta_{S'} + \frac{D_{AB}}{2}\mu_S^{(1)2}\mu_{S'}^{(1)3}\mu_{S'}^{(3)}X_{S'S'S'S}(t;\tau+\tau',\tau+\tau'+\tau'',\tau+\tau' \\
& + \tau''')\cos\theta_S\cos^3\theta_{S'} + \frac{D_{AB}}{2}\mu_S^{(1)3}\mu_S^{(3)}\mu_{S'}^{(1)2}X_{S'S'SS}(t;\tau,\tau',\tau'+\tau''')\cos^3\theta_S\cos\theta_{S'} + \frac{1}{2}\mu_S^{(1)}\mu_S^{(2)}[\mu_S^{(1)2}V_S^{(3)}X_{SSSS}(t;\tau,\tau \\
& + \tau'+\tau'',\tau+\tau'+\tau''')\cos^2\theta_S + \mu_{S'}^{(1)2}V_{S'S'}^{(3)}X_{S'S'SS}(t;\tau,\tau+\tau'+\tau'',\tau+\tau'+\tau''')\cos^2\theta_{S'} \\
& + 2\mu_S^{(1)}\mu_{S'}^{(1)}V_{S'S'}^{(3)}X_{S'S'SS}(t;\tau,\tau+\tau'+\tau'',\tau+\tau'+\tau''')\cos\theta_S\cos\theta_{S'}]\cos^2\theta_S + V_{S'S'}^{(3)}\mu_S^{(1)2}\mu_{S'}^{(1)}[\mu_S^{(2)}X_{S'S'SS}(t;\tau+\tau',\tau \\
& + \tau'',\tau+\tau'+\tau''')\cos\theta_S + \mu_{S'}^{(2)}X_{SSS'S}(t;\tau+\tau',\tau+\tau'',\tau+\tau'+\tau''')\cos\theta_{S'}]\cos^2\theta_S\cos\theta_{S'} + \frac{1}{6}\mu_S^{(1)} \\
& \times [\mu_S^{(1)3}V_S^{(4)}X_{SSSS}(t;\tau+\tau',\tau+\tau'',\tau+\tau''')\cos^3\theta_S + \mu_{S'}^{(1)3}V_{S'S'}^{(4)}X_{S'S'S'S}(t;\tau+\tau',\tau+\tau'',\tau+\tau''')\cos^3\theta_{S'} \\
& + 3\mu_S^{(1)2}\mu_{S'}^{(1)}V_{S'S'}^{(4)}X_{S'S'SS}(t;\tau+\tau',\tau+\tau'',\tau+\tau''')\cos^2\theta_S\cos\theta_{S'} + 3\mu_S^{(1)}\mu_{S'}^{(1)2}V_{S'S'}^{(4)}X_{S'S'SS}(t;\tau+\tau',\tau+\tau'',\tau \\
& + \tau''')\cos\theta_S\cos^2\theta_{S'}]\cos\theta_S, \tag{D1}
\end{aligned}$$

where we introduced the following expressions:

$$\begin{aligned}
K_{S'S'S}(t) & \equiv \int d\tau \int d\tau' \int d\tau'' E_{\text{ex}}(t-\tau)E_{\text{ex}}(t-\tau-\tau') \\
& \times E_{\text{ex}}(t-\tau-\tau'-\tau'') \times D_{S''}(\tau'')D_{S'}(\tau')D_S(\tau), \tag{D2}
\end{aligned}$$

$$\begin{aligned}
M_{S'S'S}(t) & \equiv \int d\tau \int d\tau' \int d\tau'' E_{\text{ex}}(t-\tau)E_{\text{ex}}(t-\tau-\tau') \\
& \times E_{\text{ex}}(t-\tau-\tau'') \times D_{S''}(\tau'')D_{S'}(\tau')D_S(\tau), \tag{D3}
\end{aligned}$$

$$\begin{aligned}
O_{S'S'S}(t) & \equiv \int d\tau \int d\tau' \int d\tau'' E_{\text{ex}}(t-\tau)E_{\text{ex}}(t-\tau') \\
& \times E_{\text{ex}}(t-\tau'')D_{S''}(\tau'')D_{S'}(\tau')D_S(\tau), \tag{D4}
\end{aligned}$$

$$\begin{aligned}
W_{S'S'S}(t) & \equiv \int d\tau \int d\tau' \int d\tau'' E_{\text{ex}}(t-\tau)E_{\text{ex}}(t-\tau') \\
& \times E_{\text{ex}}(t-\tau'-\tau'')D_{S''}(\tau'')D_{S'}(\tau')D_S(\tau), \tag{D5}
\end{aligned}$$

and

$$\begin{aligned}
X_{S''S''S'S}(t;\tau_\alpha,\tau_\beta,\tau_\gamma) & \equiv \int d\tau \int d\tau' \int d\tau'' \int d\tau''' \\
& \times E_{\text{ex}}(t-\tau_\alpha)E_{\text{ex}}(t-\tau_\beta)E_{\text{ex}}(t-\tau_\gamma) \\
& \times D_{S''}(\tau''')D_{S''}(\tau'')D_{S'}(\tau')D_S(\tau). \tag{D6}
\end{aligned}$$

The insertion of expression (54) into the above leads to the third-order dipole moment  $\mu_{32}^{\text{tot}(3)}(T_{123})$  which is explicitly written in our Technical Note.

#### APPENDIX E: EACH CONTRIBUTION TO THE THIRD-ORDER RESPONSE FUNCTION $R^{(3)}(T_1, T_2, T_3)$

The effect of the nonlinearity of dipole moments to  $R^{(3)}(T_1, T_2, T_3)$  becomes

$$\begin{aligned}
N^{(3)}(T_1, T_2, T_3) & \equiv \mu_A^{(1)2}\mu_A^{(2)2}Y_{AAA}(T_1, T_2, T_3)\cos^4\psi \\
& + \mu_B^{(1)2}\mu_B^{(2)2}Y_{BBB}(T_1, T_2, T_3)\cos^4\phi \\
& + \mu_A^{(1)3}\mu_A^{(3)}\{Y_{AAA}(T_{12}, T_2, T_3) \\
& + Y_{AAA}(T_{123}, T_{23}, T_3)\}\cos^4\psi + \mu_B^{(1)3}\mu_B^{(3)} \\
& \times \{Y_{BBB}(T_{12}, T_2, T_3) \\
& + Y_{BBB}(T_{123}, T_{23}, T_3)\}\cos^4\phi, \tag{E1}
\end{aligned}$$

where we have introduced  $T_{23} \equiv T_2 + T_3$  and the following expression:

$$Y_{SS'S''}(T_\alpha, T_\beta, T_\gamma) \equiv D_S(T_\alpha)D_{S'}(T_\beta)D_{S''}(T_\gamma). \quad (\text{E2})$$

That of the DID interaction leads to

$$\begin{aligned} T^{(3)}(T_1, T_2, T_3) \equiv & \frac{\tilde{T}_{AB}}{2} \mu_A^{(1)} \mu_A^{(2)} (2\mu_A^{(1)} \Phi_{AB}^{(2,0)} + 3\mu_A^{(2)} \Phi_{AB}^{(1,0)}) Y_{AAA}(T_1, T_2, T_3) \cos^3 \psi + \frac{\tilde{T}_{AB}}{2} \mu_B^{(1)} \mu_B^{(2)} (2\mu_B^{(1)} \Phi_{BA}^{(2,0)} \\ & + 3\mu_B^{(2)} \Phi_{BA}^{(1,0)}) Y_{BBB}(T_1, T_2, T_3) \cos^3 \phi + \frac{\tilde{T}_{AB}}{2} \Phi_{AB}^{(1,1)} \mu_A^{(1)} \mu_A^{(2)} \mu_B^{(1)} Y_{BAA}(T_1, T_2, T_3) \cos^2 \psi \cos \phi \\ & + \frac{\tilde{T}_{AB}}{2} \Phi_{AB}^{(1,1)} \mu_B^{(1)} \mu_B^{(2)} \mu_A^{(1)} Y_{ABB}(T_1, T_2, T_3) \cos \psi \cos^2 \phi + \frac{\tilde{T}_{AB}}{2} \Phi_{AB}^{(1,1)} \mu_A^{(1)} \mu_B^{(1)} \mu_B^{(2)} Y_{BBA}(T_1, T_2, T_3) \cos \psi \cos^2 \phi \\ & + \frac{\tilde{T}_{AB}}{2} \Phi_{AB}^{(1,1)} \mu_B^{(1)} \mu_A^{(1)} \mu_A^{(2)} Y_{AAB}(T_1, T_2, T_3) \cos^2 \psi \cos \phi + \frac{\tilde{T}_{AB}}{2} \mu_A^{(1)2} (4\mu_A^{(3)} \Phi_{AB}^{(1,0)} \\ & + \mu_A^{(1)} \Phi_{AB}^{(3,0)}) Y_{AAA}(T_{123}, T_{23}, T_3) \cos^3 \psi + \frac{\tilde{T}_{AB}}{2} \mu_B^{(1)2} (4\mu_B^{(3)} \Phi_{BA}^{(1,0)} + \mu_B^{(1)} \Phi_{BA}^{(3,0)}) Y_{BBB}(T_{123}, T_{23}, T_3) \cos^3 \phi \\ & + \frac{\tilde{T}_{AB}}{2} \mu_A^{(1)2} (4\mu_A^{(3)} \Phi_{AB}^{(1,0)} + \mu_A^{(1)} \Phi_{AB}^{(3,0)}) Y_{AAA}(T_{12}, T_2, T_3) \cos^3 \psi + \frac{\tilde{T}_{AB}}{2} \mu_B^{(1)2} (4\mu_B^{(3)} \Phi_{BA}^{(1,0)} \\ & + \mu_B^{(1)} \Phi_{BA}^{(3,0)}) Y_{BBB}(T_{12}, T_2, T_3) \cos^3 \phi + \frac{\tilde{T}_{AB}}{2} [\mu_A^{(1)} \mu_B^{(1)2} \Phi_{AB}^{(1,2)} Y_{BBA}(T_{12}, T_2, T_3) \cos \psi \cos^2 \phi + \mu_A^{(1)2} \mu_B^{(1)} \Phi_{AB}^{(2,1)} \\ & \times \{Y_{ABA}(T_{12}, T_2, T_3) + Y_{BAA}(T_{12}, T_2, T_3)\} \cos^2 \psi \cos \phi] + \frac{\tilde{T}_{AB}}{2} [\mu_B^{(1)} \mu_A^{(1)2} \Phi_{AB}^{(2,1)} Y_{AAB}(T_{12}, T_2, T_3) \cos^2 \psi \cos \phi \\ & + \mu_B^{(1)2} \mu_A^{(1)} \Phi_{AB}^{(1,2)} \{Y_{BAB}(T_{12}, T_2, T_3) + Y_{ABB}(T_{12}, T_2, T_3)\} \cos \psi \cos^2 \phi] + \tilde{T}_{AB} \alpha_A^{(1)} \mu_A^{(1)} \mu_B^{(1)2} \mu_B^{(2)} \\ & \times \{Y_{BBA}(T_1, T_{23}, T_3) + Y_{ABB}(T_{123}, T_2, T_3) + Y_{BAB}(T_{12}, T_{23}, T_3) + Y_{ABB}(T_{123}, T_{23}, T_3) + Y_{BAB}(T_{123}, T_{23}, T_3) \\ & + Y_{BBA}(T_{123}, T_{23}, T_3)\} \cos \psi \cos^2 \phi + \tilde{T}_{AB} \alpha_B^{(1)} \mu_B^{(1)} \mu_A^{(1)2} \mu_A^{(2)} \{Y_{AAB}(T_1, T_{23}, T_3) + Y_{BAA}(T_{123}, T_2, T_3) \\ & + Y_{ABA}(T_{12}, T_{23}, T_3) + Y_{BAA}(T_{123}, T_{23}, T_3) + Y_{ABA}(T_{123}, T_{23}, T_3) + Y_{AAB}(T_{123}, T_{23}, T_3)\} \cos^2 \psi \cos \phi \\ & + \tilde{T}_{AB} \alpha_A^{(1)} \mu_A^{(1)} \mu_B^{(1)2} \mu_B^{(2)} \{Y_{AAB}(T_1, T_{23}, T_3) + Y_{BAA}(T_{123}, T_2, T_3) + Y_{ABA}(T_{12}, T_{23}, T_3)\} \cos^2 \psi \cos \phi \\ & + \tilde{T}_{AB} \alpha_B^{(1)} \mu_B^{(1)} \mu_B^{(2)} \mu_A^{(1)2} \{Y_{BBA}(T_1, T_{23}, T_3) + Y_{ABB}(T_{123}, T_2, T_3) + Y_{BAB}(T_{12}, T_{23}, T_3)\} \cos \psi \cos^2 \phi \\ & + \tilde{T}_{AB} \mu_A^{(1)2} \alpha_A^{(2)} \mu_B^{(1)2} \{Y_{BAA}(T_{123}, T_{23}, T_3) + Y_{ABA}(T_{123}, T_{23}, T_3) + Y_{AAB}(T_{123}, T_{23}, T_3)\} \cos^2 \psi \cos \phi \\ & + \tilde{T}_{AB} \mu_B^{(1)2} \alpha_B^{(2)} \mu_A^{(1)2} \{Y_{ABB}(T_{123}, T_{23}, T_3) + Y_{BAB}(T_{123}, T_{23}, T_3) + Y_{BBA}(T_{123}, T_{23}, T_3)\} \cos \psi \cos^2 \phi. \quad (\text{E3}) \end{aligned}$$

The contribution of the DD interaction is calculated as

$$\begin{aligned} D^{(3)}(T_1, T_2, T_3) \equiv & \tilde{D}_{AB} \mu_A^{(1)2} \mu_A^{(2)2} \mu_B^{(1)2} [Z_{AA}(T_1, T_2, T_3) + L_{AAB}(T_{23}, T_3) D_A(T_1) + L_{ABA}(T_{23}, T_3) D_A(T_{12}) + L_{ABA}(T_{123}, T_3) D_A(T_2) \\ & + H_{ABA}(T_1, T_2) D_A(T_3)] \cos^3 \psi \cos \phi + \tilde{D}_{AB} \mu_B^{(1)2} \mu_B^{(2)2} \mu_A^{(1)2} [Z_{BB}(T_1, T_2, T_3) + L_{BBA}(T_{23}, T_3) D_B(T_1) \\ & + L_{BAB}(T_{23}, T_3) D_B(T_{12}) + L_{BAB}(T_{123}, T_3) D_B(T_2) + H_{BAB}(T_1, T_2) D_B(T_3)] \cos \psi \cos^3 \phi \\ & + \tilde{D}_{AB} \mu_A^{(1)2} \mu_A^{(2)} \mu_B^{(1)2} \mu_B^{(2)} \left[ \frac{1}{2} H_{BBA}(T_1, T_2) D_A(T_3) + L_{ABA}(T_{23}, T_3) D_B(T_1) + L_{AAB}(T_{23}, T_3) D_B(T_{12}) \right. \\ & + L_{AAB}(T_{123}, T_3) D_B(T_2) + Z_{BA}(T_2, T_1, T_3) + N_{AABB}(T_3, T_{23}, T_{123}) + N_{ABAB}(T_3, T_{23}, T_{123}) \\ & \left. + N_{ABBA}(T_3, T_{23}, T_{123}) \right] \cos^2 \psi \cos^2 \phi + \tilde{D}_{AB} \mu_B^{(1)2} \mu_B^{(2)} \mu_A^{(1)2} \mu_A^{(2)} \left[ \frac{1}{2} H_{AAB}(T_1, T_2) D_B(T_3) + L_{BAB}(T_{23}, T_3) D_A(T_1) \right. \\ & + L_{BBA}(T_{23}, T_3) D_A(T_{12}) + L_{BBA}(T_{123}, T_3) D_A(T_2) + Z_{AB}(T_2, T_1, T_3) + N_{BBAA}(T_3, T_{23}, T_{123}) \\ & \left. + N_{BABA}(T_3, T_{23}, T_{123}) + N_{BAAB}(T_3, T_{23}, T_{123}) \right] \cos^2 \psi \cos^2 \phi \\ & + \tilde{D}_{AB} \mu_A^{(1)2} \mu_B^{(1)3} \mu_B^{(3)} Z_{BB}(T_3, T_{12}, T_2) \cos \psi \cos^3 \phi + \tilde{D}_{AB} \mu_B^{(1)2} \mu_A^{(1)3} \mu_A^{(3)} Z_{AA}(T_3, T_{12}, T_2) \cos^3 \psi \cos \phi \\ & + \tilde{D}_{AB} \mu_A^{(1)3} \mu_B^{(1)2} \mu_A^{(3)} \cos^3 \psi \cos \phi [Z_{AA}(T_{12}, T_2, T_3) + Z_{AA}(T_2, T_{12}, T_3) + Z_{AA}(T_3, T_{123}, T_{23})] \end{aligned}$$



$$\begin{aligned}
& + Z_{AA}(T_{23}, T_{123}, T_3) + Z_{AA}(T_{123}, T_{23}, T_3)] + \tilde{D}_{AB}\mu_B^{(1)3}\mu_A^{(1)2}\mu_B^{(3)}\cos\psi\cos^3\phi[Z_{BB}(T_{12}, T_2, T_3) \\
& + Z_{BB}(T_2, T_{12}, T_3) + Z_{BB}(T_3, T_{123}, T_{23}) + Z_{BB}(T_{23}, T_{123}, T_3) + Z_{BB}(T_{123}, T_{23}, T_3)] \\
& + \tilde{D}_{AB}\mu_A^{(1)2}\mu_B^{(1)2}\mu_B^{(2)2}Z_{BB}(T_3, T_1, T_2)\cos\psi\cos^3\phi + \tilde{D}_{AB}\mu_B^{(1)2}\mu_A^{(1)2}\mu_A^{(2)2}Z_{AA}(T_3, T_1, T_2)\cos^3\psi\cos\phi, \quad (E4)
\end{aligned}$$

where

$$Z_{SS'}(T_\alpha, T_\beta, T_\gamma) \equiv G_{AB}(T_\alpha)D_S(T_\beta)D_{S'}(T_\gamma). \quad (E5)$$

We have also introduced

$$L_{S,S',S''}(T_\alpha, T_\beta) \equiv \int d\tau D_S(\tau)D_{S'}(T_\alpha - \tau)D_{S''}(T_\beta - \tau) \quad (E6)$$

and

$$N_{S,S',S'',S'''}(T_\alpha, T_\beta, T_\gamma) \equiv \int d\tau D_S(\tau)D_{S'}(T_\alpha - \tau)D_{S''}(T_\beta - \tau)D_{S'''}(T_\gamma - \tau). \quad (E7)$$

Their explicit integrated forms are given in our web page.<sup>42</sup> The effect of the anharmonicity becomes

$$\begin{aligned}
A^{(3)}(T_1, T_2, T_3) & \equiv \frac{1}{2}\mu_A^{(1)}\mu_A^{(2)}[\mu_A^{(1)2}V_A^{(3)}H_{AAA}(T_1, T_2)\cos^2\psi + \mu_B^{(1)2}V_{AB}^{(3)}H_{BBA}(T_1, T_2)\cos^2\phi \\
& + \mu_A^{(1)}\mu_B^{(1)}V_{BA}^{(3)}H_{ABA}(T_1, T_2)\cos\psi\cos\phi]D_A(T_3)\cos^2\psi + \frac{1}{2}\mu_B^{(1)}\mu_B^{(2)}[\mu_B^{(1)2}V_B^{(3)}H_{BBB}(T_1, T_2)\cos^2\phi \\
& + \mu_A^{(1)2}V_{BA}^{(3)}H_{AAB}(T_1, T_2)\cos^2\psi + \mu_B^{(1)}\mu_A^{(1)}V_{AB}^{(3)}H_{BAB}(T_1, T_2)\cos\psi\cos\phi]D_B(T_3)\cos^2\phi \\
& + \mu_A^{(1)2}\mu_B^{(2)}\mu_B^{(1)}V_{BA}^{(3)}\cos^3\psi\cos\phi[L_{AAB}(T_{123}, T_3)D_B(T_2) + L_{AAB}(T_{23}, T_3)D_B(T_{12}) + L_{ABA}(T_{23}, T_3)D_B(T_1)] \\
& + \mu_B^{(1)2}\mu_B^{(2)}\mu_A^{(1)}V_{AB}^{(3)}\cos\psi\cos^3\phi[L_{BBA}(T_{123}, T_3)D_A(T_2) + L_{BBA}(T_{23}, T_3)D_A(T_{12}) + L_{BAB}(T_{23}, T_3)D_A(T_1)] \\
& + \mu_A^{(1)2}\mu_B^{(2)}\mu_B^{(1)}V_{BA}^{(3)}\cos^2\psi\cos^2\phi[L_{ABA}(T_{123}, T_3)D_A(T_2) + L_{ABA}(T_{23}, T_3)D_A(T_{12}) + L_{AAB}(T_{23}, T_3)D_A(T_1)] \\
& + \mu_B^{(1)2}\mu_A^{(2)}\mu_A^{(1)}V_{AB}^{(3)}\cos^2\psi\cos^2\phi[L_{BAB}(T_{123}, T_3)D_B(T_2) + L_{BAB}(T_{23}, T_3)D_B(T_{12}) + L_{BBA}(T_{23}, T_3)D_B(T_1)] \\
& + \mu_A^{(1)4}V_A^{(4)}N_{AAAA}(T_3, T_{23}, T_{123})\cos^4\psi + \mu_B^{(1)4}V_B^{(4)}N_{BBBB}(T_3, T_{23}, T_{123})\cos^4\phi \\
& + \mu_A^{(1)}\mu_B^{(1)3}V_{AB}^{(4)}N_{ABBB}(T_3, T_{23}, T_{123})\cos\psi\cos^3\phi + \mu_B^{(1)}\mu_A^{(1)3}V_{BA}^{(4)}N_{BAAA}(T_3, T_{23}, T_{123})\cos^3\psi\cos\phi \\
& + \mu_A^{(1)3}\mu_B^{(1)}V_{BA}^{(4)}\cos^3\psi\cos\phi[N_{AAAB}(T_3, T_{23}, T_{123}) + N_{AABA}(T_3, T_{23}, T_{123}) + N_{ABAA}(T_3, T_{23}, T_{123})] \\
& + \mu_B^{(1)3}\mu_A^{(1)}V_{AB}^{(4)}\cos\psi\cos^3\phi[N_{BBBA}(T_3, T_{23}, T_{123}) + N_{BBAB}(T_3, T_{23}, T_{123}) + N_{BABB}(T_3, T_{23}, T_{123})] \\
& + \mu_A^{(1)2}\mu_B^{(1)2}V_{AB}^{(4)}\cos^2\psi\cos^2\phi[N_{ABBA}(T_3, T_{23}, T_{123}) + N_{ABAB}(T_3, T_{23}, T_{123}) + N_{AABB}(T_3, T_{23}, T_{123})] \\
& + \mu_B^{(1)2}\mu_A^{(1)2}V_{BA}^{(4)}\cos^2\psi\cos^2\phi[N_{BAAB}(T_3, T_{23}, T_{123}) + N_{BABA}(T_3, T_{23}, T_{123}) + N_{BBAA}(T_3, T_{23}, T_{123})]. \quad (E8)
\end{aligned}$$

<sup>1</sup> Y. Tanimura and S. Mukamel, J. Chem. Phys. **99**, 9496 (1993).

<sup>2</sup> V. Astinov, K. J. Kubarych, C. J. Milne, and R. J. D. Miller, Chem. Phys. Lett. **327**, 334 (2000); K. J. Kubarych, C. L. Milne, S. Lin, V. Astinov, and J. D. Miller, J. Chem. Phys. **116**, 2016 (2002).

<sup>3</sup> L. J. Kaufman, J. Heo, L. D. Ziegler, and G. R. Fleming, Phys. Rev. Lett. **88**, 207402 (2002); L. J. Kaufman, D. A. Blank, and G. R. Fleming, J. Chem. Phys. **114**, 2312 (2001); D. A. Blank, L. J. Kaufman, and G. R. Fleming, J. Chem. Phys. **113**, 771 (2000); **111**, 3105 (1999).

<sup>4</sup> S. Saito and I. Ohmine, Phys. Rev. Lett. **88**, 207401 (2002); J. Chem. Phys. **119**, 9073 (2003).

<sup>5</sup> P. Hamm, M. Lim, and R. M. Hochstrasser, J. Phys. Chem. B **102**, 6123 (1998); M. T. Zanni, S. Gnanakaran, J. Stenger, and R. M. Hochstrasser, *ibid.* **105**, 6520 (2001); S. Gnanakaran and R. M. Hochstrasser, J. Am. Chem. Soc. **123**, 12886 (2001).

<sup>6</sup> M. Khalil, N. Demirdoven, and A. Tokmakoff, J. Phys. Chem. A **107**, 5258 (2003).

<sup>7</sup> K. Ohta, H. Maekawa, S. Saito, and K. Tominaga, J. Phys. Chem. A **107**, 5643 (2003); K. Ohta, H. Maekawa, and K. Tominaga, Chem. Phys. Lett. **386**, 32 (2004); J. Phys. Chem. A **108**, 1333 (2004); H. Maekawa, K. Ohta, and K. Tominaga, Phys. Chem. Chem. Phys. **6**, 4074 (2004).

<sup>8</sup> K. Okumura and Y. Tanimura, J. Chem. Phys. **106**, 1687 (1997).

<sup>9</sup> T. Steffen and Y. Tanimura, J. Phys. Soc. Jpn. **69**, 3115 (2000); Y. Tanimura and T. Steffen, *ibid.* **69**, 4095 (2000).

<sup>10</sup> P. Mukherjee, A. T. Krummel, E. C. Fulmer, I. Kass, I. T. Arkin, and M. T. Zanni, J. Chem. Phys. **120**, 10215 (2004).

<sup>11</sup> P. Hamm, M. Lim, W. F. DeGrado, and R. M. Hochstrasser, J. Chem. Phys. **112**, 1907 (2000).

<sup>12</sup> M. C. Asplund, M. T. Zanni, and R. M. Hochstrasser, Proc. Natl. Acad. Sci. U.S.A. **97**, 8219 (2000).

<sup>13</sup> P. Hamm, M. Lim, W. F. DeGrado, and R. M. Hochstrasser, Proc. Natl. Acad. Sci. U.S.A. **96**, 2036 (1999).

<sup>14</sup> H. S. Chung, M. Khalil, and A. Tokmakoff, J. Phys. Chem. B **108**, 15332 (2004).

<sup>15</sup> N. Demirdöven, C. M. Cheatum, H. S. Chung, M. Khalil, J. Knoester, and A. Tokmakoff, J. Am. Chem. Soc. **126**, 7981 (2004).

<sup>16</sup> I. V. Rubtsov, K. Kumar, and R. M. Hochstrasser, Chem. Phys. Lett. **402**, 439 (2005).

<sup>17</sup> S. Woutersen, Y. Mu, G. Stock, and P. Hamm, Chem. Phys. **266**, 137 (2001).

<sup>18</sup> J. B. Asbury, T. Steinel, and M. D. Fayer, J. Phys. Chem. B **108**, 6544 (2004); J. B. Asbury, T. Steinel, C. Stromberg, S. A. Corcelli, C. P.

- Lawrence, J. L. Skinner, and M. D. Fayer, *J. Phys. Chem. A* **108**, 1107 (2004).
- <sup>19</sup>C. J. Fecko, J. D. Eaves, J. Loparo, A. Tokmakoff, and P. L. Geissler, *Science* **301**, 1698 (2003).
- <sup>20</sup>T. Kato and Y. Tanimura, *Chem. Phys. Lett.* **341**, 329 (2001).
- <sup>21</sup>Y. Suzuki and Y. Tanimura, *J. Chem. Phys.* **119**, 1650 (2003).
- <sup>22</sup>T. Kato and Y. Tanimura, *J. Chem. Phys.* **120**, 260 (2004).
- <sup>23</sup>A. Ishizaki and Y. Tanimura, *J. Chem. Phys.* **123**, 14503 (2005).
- <sup>24</sup>M. Cho, *Phys. Rev. A* **61**, 023406 (2000).
- <sup>25</sup>K. Park and M. Cho, *J. Chem. Phys.* **112**, 5021 (2000).
- <sup>26</sup>K. Okumura, D. M. Jonas, and Y. Tanimura, *Chem. Phys.* **266**, 237 (2001).
- <sup>27</sup>K. Okumura, A. Tokmakoff, and Y. Tanimura, *J. Chem. Phys.* **111**, 492 (1999).
- <sup>28</sup>M. Cho, D. A. Blank, J. Sung, K. Park, S. Hahn, and G. R. Fleming, *J. Chem. Phys.* **112**, 2082 (2000).
- <sup>29</sup>A. M. Moran, S.-M. Park, J. Dreyer, and S. Mukamel, *J. Chem. Phys.* **118**, 3651 (2003).
- <sup>30</sup>A. Piryatinski, S. Tretiak, V. Chernyak, and S. Mukamel, *J. Raman Spectrosc.* **31**, 125 (2000).
- <sup>31</sup>K. Kwac and M. Cho, *J. Chem. Phys.* **119**, 2256 (2003).
- <sup>32</sup>C. Scheurer, A. Piryatinski, and S. Mukamel, *J. Am. Chem. Soc.* **123**, 3114 (2001).
- <sup>33</sup>W. Zhuang, D. Abramavicius, and S. Mukamel, *Proc. Natl. Acad. Sci. U.S.A.* **102**, 7443 (2005).
- <sup>34</sup>S. Hahn, K. Kwak, and M. Cho, *J. Chem. Phys.* **112**, 4553 (2000).
- <sup>35</sup>K. F. Everitt and J. L. Skinner, *Chem. Phys.* **266**, 197 (2001); K. F. Everitt, E. Geva, and J. L. Skinner, *J. Chem. Phys.* **114**, 1326 (2001); A. Piryatinski and J. L. Skinner, *J. Phys. Chem. B* **106**, 8055 (2002); A. Piryatinski, C. P. Lawrence, and J. L. Skinner, *J. Chem. Phys.* **118**, 9664 (2003); **118**, 9672 (2003).
- <sup>36</sup>W. G. Noid, G. S. Ezra, and R. F. Loring, *J. Phys. Chem. B* **108**, 6536 (2004); *J. Chem. Phys.* **120**, 1491 (2004); K. A. Merchant, W. G. Noid, D. E. Thompson, R. Akiyama, R. F. Loring, and M. D. Fayer, *J. Phys. Chem. B* **107**, 4 (2003).
- <sup>37</sup>C. Scheurer and S. Mukamel, *J. Chem. Phys.* **116**, 6803 (2002).
- <sup>38</sup>W. M. Zhang, V. Chernyak, and S. Mukamel, *J. Chem. Phys.* **110**, 5011 (1999).
- <sup>39</sup>C. M. Cheatum, A. Tokmakoff, and J. Knoester, *J. Chem. Phys.* **120**, 8201 (2004).
- <sup>40</sup>O. Golonzka and A. Tokmakoff, *J. Chem. Phys.* **115**, 297 (2001).
- <sup>41</sup>O. Golonzka, M. Khalil, N. Demirdöven, and A. Tokmakoff, *J. Chem. Phys.* **115**, 10814 (2001).
- <sup>42</sup><http://theochem.kuchem.kyoto-u.ac.jp/members/kim.htm>
- <sup>43</sup>J. D. Jackson, *Classical Electrodynamics* (Wiley, New York, 1999).
- <sup>44</sup>M. Khalil and A. Tokmakoff, *Chem. Phys.* **266**, 213 (2001).
- <sup>45</sup>S. Mukamel, *Principles of Nonlinear Optical Spectroscopy* (Oxford University Press, New York, 1995).
- <sup>46</sup>K. Scanlon, R. A. Eades, and D. A. Dixon, *Spectrochim. Acta, Part A* **38**, 849 (1982).
- <sup>47</sup>H. Torii, *Chem. Phys. Lett.* **353**, 431 (2002).
- <sup>48</sup>M. Cho, *J. Chem. Phys.* **112**, 9002 (2000).
- <sup>49</sup>K. Park and M. Cho, *J. Chem. Phys.* **109**, 10559 (1998).
- <sup>50</sup>M. Cho, K. Okumura, and Y. Tanimura, *J. Chem. Phys.* **108**, 1326 (1998).
- <sup>51</sup>J. Sung and M. Cho, *J. Chem. Phys.* **113**, 7072 (2000).
- <sup>52</sup>K. Park and M. Cho, *J. Chem. Phys.* **112**, 10496 (2000).
- <sup>53</sup>J. Sung, R. J. Silbey, and M. Cho, *J. Chem. Phys.* **115**, 1422 (2001).
- <sup>54</sup>K. Okumura and Y. Tanimura, *Chem. Phys. Lett.* **278**, 175 (1997).
- <sup>55</sup>Y. Tanimura and P. G. Wolynes, *Phys. Rev. A* **43**, 4131 (1991).
- <sup>56</sup>W. G. Noid and R. F. Loring, *J. Chem. Phys.* **121**, 7057 (2004).
- <sup>57</sup>K. Okumura and Y. Tanimura, *Phys. Rev. E* **56**, 2747 (1997).